

12-2010

## Effects of Combined Bevacizumab and Paclitaxel on Tumor Interstitial Fluid Pressure in a Preclinical Breast Cancer Model

Ricardo Hugo Alvarez

Follow this and additional works at: [https://digitalcommons.library.tmc.edu/utgsbs\\_dissertations](https://digitalcommons.library.tmc.edu/utgsbs_dissertations)



Part of the [Medicine and Health Sciences Commons](#)

### Recommended Citation

Alvarez, Ricardo Hugo, "Effects of Combined Bevacizumab and Paclitaxel on Tumor Interstitial Fluid Pressure in a Preclinical Breast Cancer Model" (2010). *The University of Texas MD Anderson Cancer Center UTHealth Graduate School of Biomedical Sciences Dissertations and Theses (Open Access)*. 104. [https://digitalcommons.library.tmc.edu/utgsbs\\_dissertations/104](https://digitalcommons.library.tmc.edu/utgsbs_dissertations/104)

This Thesis (MS) is brought to you for free and open access by the The University of Texas MD Anderson Cancer Center UTHealth Graduate School of Biomedical Sciences at DigitalCommons@TMC. It has been accepted for inclusion in The University of Texas MD Anderson Cancer Center UTHealth Graduate School of Biomedical Sciences Dissertations and Theses (Open Access) by an authorized administrator of DigitalCommons@TMC. For more information, please contact [digitalcommons@library.tmc.edu](mailto:digitalcommons@library.tmc.edu).

Effects of Combined Bevacizumab and Paclitaxel on Tumor Interstitial Fluid Pressure in a  
Preclinical Breast Cancer Model

By

Ricardo H. Alvarez, M.D.

APPROVED:

---

Janet E. Price, D Phil

---

Douglas D. Boyd, Ph D

---

Francisco J. Esteva, MD, Ph D.

---

Karin Hahn, MD, MSc, MPH

---

Vicente Valero, M.D.

APPROVED:

---

Dean, The University of Texas

Health Science Center at Houston

Graduate School of Biomedical Sciences

**EFFECTS OF COMBINED BEVACIZUMAB AND PACLITAXEL ON TUMOR  
INTERSTITIAL FLUID PRESSURE IN A PRECLINICAL BREAST CANCER  
MODEL**

**A  
THESIS**

**Presented to the Faculty of the University of Texas**

**Health Science Center at Houston**

**And**

**The University of Texas**

**M. D. Anderson Cancer Center**

**Graduate School of Biomedical Sciences**

**In Partial Fulfillment**

**of the Requirements**

**For the Degree of**

**MASTER OF SCIENCE**

**Program in Human Biology and Patient-Based Research**

**By**

**Ricardo H. Alvarez, M.D.**

**Houston, Texas**

**December, 2010**

## **DEDICATION**

I want to dedicate my thesis to my wife Gloria, and my sons, Ignacio and Ernesto.

## **ACKNOWLEDGMENTS**

I want thank to Dr. Janet E. Price for her constant supervision, guidance and support during this thesis work.

I thank Dr. Vicente Valero as my clinical mentor during the last three years and Dr Gabriel N. Hortobagyi for his support and provide me with the time and resources to carry on the experiments.

I thank Dr. Emil Freireich, for his enthusiasm to do clinical research and Dr. Waun K. Hong for being a role model for many fellows at MD Anderson Cancer Center.

I also want to thank Galina Kiriakova, for her assistance in the animal facility, and Donna Reynolds from the Histology Laboratory at Cancer Biology.

## **ABSTRACT**

### **Effects of Combined Bevacizumab and Paclitaxel on Tumor Interstitial Fluid Pressure in a Preclinical Breast Cancer Model**

by

Ricardo H. Alvarez

Several mechanisms of cell resistance are often accountable for unsuccessful chemotherapy against cancer. Another reason, which has received increased attention, is the inefficient transport of anticancer drugs into tumor tissue. These impaired transports of chemotherapy into the tumor have been attributed to abnormal microvasculature and to pathologically increased tumor hypertension also called: interstitial fluid pressure (IFP). The pathophysiological processes leading to elevated tumor IFP are poorly understood. Here, in a preclinical breast cancer model, it is argued that a condition of raised IFP is a major factor in preventing optimal access of systemically administered chemotherapy agents. In our experimental model, we used a GILM2 human breast cancer in xenografts; mice were treated with different doses of paclitaxel –a widely used antimicrotubular agent, and bevacizumab – monoclonal antibody against vascular endothelial growth factor (VEGF). The proposed research project is designed to test the hypothesis that paclitaxel in combination with bevacizumab decreases the tumor IPF by restoring tumor permeability and increasing chemotherapy delivery. We demonstrated that the combination of paclitaxel and bevacizumab produced greater tumor control than either agent given alone and this combination reduced the IFP, producing an increment of 75% of apoptosis compared with the control arm. In addition, the intra-tumor paclitaxel quantification by liquid chromatography/Mass Spectrometry (LC/MS) demonstrated that lower dose of both agents showed a synergistic effect compared with high dose of treatment, where there is no significantly increase of paclitaxel into the tumor. These preclinical results are likely to have broad implications for the utility of anti-angiogenic therapies alone and in combination with chemotherapeutic agents.

## TABLE OF CONTENTS

<b>DEDICATION.....</b>	<b>III</b>
<b>ACKNOWLEDGMENTS .....</b>	<b>IV</b>
<b>ABSTRACT.....</b>	<b>V</b>
<b>LIST OF ILLUSTRATIONS.....</b>	<b>VIII</b>
<b>LIST OF ABBREVIATIONS .....</b>	<b>IX</b>
<b>CHAPTER 1 .....</b>	<b>1</b>
1. Introduction: Breast Cancer 2010 .....	1
2. Mechanism of Resistance to Cancer Treatment.....	2
3. Tumor Microenvironment .....	3
4. Stromal Microenvironment as Cause of Drug Resistance .....	8
<b>CHAPTER 2 .....</b>	<b>10</b>
1. Physiological Barriers of Drug Resistance .....	10
<i>Tumor Hypoxia</i> .....	13
<i>Tumor Acidosis</i> .....	14
<b>CHAPTER 3 .....</b>	<b>15</b>
1. Interstitial Fluid Pressure and Transvascular Transport.....	15
<i>The interstitium</i> .....	15
<i>Regulation of the IFP</i> .....	19
<i>IFP is Elevated in Solid Tumors</i> .....	19
<i>Consequences of Elevated IFP</i> .....	20
<i>Role of Platelet-Derived Growth Factor Receptor in tumor IFP Regulation</i> .....	21

<i>IFP and transvascular transport in tumors</i> .....	23
<i>Tumor Angiogenesis and Interstitial Hypertension</i> .....	24
<b>CHAPTER 4</b> .....	<b>27</b>
Investigation of Tumor IFP in a Xenograft Breast Cancer Model .....	27
Material and Methods .....	28
Statistical Analysis .....	39
Results .....	40
LC/MS Analysis .....	68
Discussion .....	71
<b>BIBLIOGRAPHY</b> .....	<b>76</b>
<b>VITA</b> .....	<b>89</b>



**LIST OF ILLUSTRATIONS**

FIGURE 1 ..... 7

FIGURE 2 ..... 11

FIGURE 3 ..... 18

FIGURE 4 ..... 31

FIGURE 5 ..... 34

FIGURE 6 ..... 41

FIGURE 7 ..... 43

FIGURE 8 ..... 49

FIGURE 9 ..... 52

FIGURE 10 ..... 57

FIGURE 11 ..... 61

FIGURE 12 ..... 65

FIGURE 13 ..... 69

## **LIST OF ABBREVIATIONS:**

IFP	Interstitial fluid pressure
VEGF	Vascular endothelial growth factor
MBC	Metastatic breast cancer
LC/MS	Liquid chromatography/mass spectrometry
ECM	Extracellular matrix
HIF-1	Hypoxia-inducible factor 1
pHe	Microenvironment tumor acidosis
pHi	Intracellular pH
GAG	Glycosaminoglycans
MVP	Microvascular pressure
VPF	Vascular permeability factor
PDGF	Platelet-derived growth factor
MFP	Mammary fat pad
LD	Low dose
HD	High dose
DCE-MRI	Dynamic-contrast enhanced magnetic resonance imaging

## Chapter 1

### 1. Introduction: Breast Cancer 2010

In the United States, breast cancer is the most commonly diagnosed cancer and is the second leading cause of death in women. <sup>[1]</sup> It is estimated that 207,090 new patients of breast cancer will be diagnosed in the United States in 2010 representing 28% of all female cancers incidence, and 39,840 deaths representing 15% of all female cancer death. <sup>[2]</sup> Breast cancer is also an important public health problem in the world; in 2007, 1.3 million women were diagnosed with breast cancer worldwide, and almost 465,000 died from the disease. <sup>[3]</sup> Over the past few years, breast cancer mortality has been steadily decreasing due to a variety of reasons, including success of mammography screening and the availability of newer cytotoxic chemotherapy and targeted agents. <sup>[4, 5]</sup>

The treatment of MBC is palliative and rarely curative. Therefore, the goals of the treatment consist in alleviation of symptoms and improvement or maintenance of good quality of life. This has led to much interest in the understanding of the pathogenesis of breast cancer metastasis and the mechanism of tumor resistance.

Although the use of anthracyclines and taxanes has led to an increase in survival of patients with metastatic or locally advanced disease, the benefit from third-line therapies is less clear. Patients who have disease that is resistant to these therapies, or who develop toxicities causing cessation, may then receive other agents that are of limited benefit. Although there is no widely accepted standard of care, current options for patients that who failed anthracyclines and taxanes include the vinca alkaloids, <sup>[6, 7]</sup> gemcitabine, <sup>[8]</sup> capecitabine, <sup>[9, 10]</sup> nanoparticle albumin-bound paclitaxel, <sup>[11]</sup> and recently, ixabepilone <sup>[12-15]</sup>

The principal cause of death from cancer is metastases that are resistant to conventional therapies. Approximately, 1 out of 5 patients with diagnosis a of breast cancer will develop metastasis in 5 years.<sup>[16]</sup> The prognosis of patients with metastatic breast cancer remains poor; the 5-year survival rate is only 26% in the United States.<sup>[17]</sup>

Because of the lack of clinical responses to anti-VEGF treatment in solid tumors, with the exception of renal cell and hepatocellular carcinoma, several investigators started combining anti-VEGF treatments with conventional cytotoxic drugs. With this combination, the aim is to target two compartments: the stroma and endothelial cells and the cancer cells.

Currently, in the United States, the Food and Drug Agency approved in three of the most common solid tumors -breast, lung and colorectal cancer- the combination of anti-VEGF (bevacizumab) in combination with chemotherapy as front-line treatment for advanced disease.

## **2. Mechanism of Resistance to Cancer Treatment**

One of the principal factors responsible for failure to respond to cancer treatment is drug resistance. There are two types of tumor resistance: a) intrinsic resistance to *de novo* treatment with chemotherapy, and b) secondary or acquired resistance, for the cases when tumor initially responded to treatment and became resistant during, or right after treatment.<sup>[18]</sup> Drug resistance, whether intrinsic or acquired, is believed to cause treatment failure in over 90% of patients with metastatic cancer, and resistant micrometastatic tumor cells may also reduce the effectiveness of chemotherapy in the adjuvant setting.<sup>[19]</sup> Clearly, if drug resistance could be overcome, the impact on survival of the cancer patient would be highly significant.

There are many factors that affect drug sensitivity. These include mechanisms such as those that limit the amount of drug reaching the tumors and those affecting the tumor microenvironment.<sup>[18]</sup> The classical description of cellular mechanisms of resistance involve multiple processes, including: drug influx and efflux, drug inactivation, drug targets, DNA damage repair, cell cycle arrest versus apoptosis, induction of apoptosis, and pro-survival signaling.<sup>[20]</sup>

### **3. Tumor Microenvironment**

More than a century ago, Stephen Paget, a British surgeon, proposed that the microenvironment of a developing tumor is a crucial regulator of carcinogenesis and he elaborated his famous “seed and soil” hypothesis.<sup>[21]</sup> He hypothesized that cancer cells (the seeds) were interconnected by several types of signals with the stroma cells (the soil). After reviewed 735 autopsies of patients with breast cancer in 1889, he concluded that the pattern of metastasis is not a random process, instead was a complex and regulated process which depends on the tumor stroma. This seminal observation was demonstrated a century later with multiple experiments.<sup>[22]</sup>

An influential publication by Dr. Dvorak in 1986, clearly showed that the growth of carcinomas beyond a diameter of about 1-2 mm requires the formation of a supporting tumor stroma to ensure the supply of nutrients for tumor cell survival and growth.<sup>[23]</sup> The tumor stroma microenvironment may differ between tumor types and disease stages. Tumor stroma represents between 20% to 50% of the mass in breast, lung, and colorectal carcinomas. However, in tumors with extensive desmoplastic component, the stroma can represent 90% of the mass of tumor.

It is important to mention that the mass and composition of the stroma differs between tumors and is not related with the degree of tumor malignancy.<sup>[24]</sup>

The tumor stroma is composed of a variety of cells which are interconnected by several types of cross-talk signaling. The most common resident cell types are fibroblast, smooth muscle cells, immune and inflammatory cells, lipocytes and endothelial cells.<sup>[25]</sup> The active interconnections between cancer cells and the tumor stroma are responsible in part for the strong influences that stroma cells impose on cancer cells. The traditional concept that cells immediately adjacent to a tumor are passive structural elements that elicit an immune response in an attempt to resist and reject the tumor has now been challenged by a considerable body of evidence from many investigators.<sup>[26]</sup> So, it is becoming apparent that the tumor microenvironment exerts an important role in the neoplastic phenotype.

In order to maintain a tissue homeostasis, all tissues require an extracellular network to provide structural support and facilitate the cell-cell communication. The microenvironment of solid tumors has several characteristics that distinguish it from the corresponding normal tissue. These characteristics are thought to become established due to an abnormal relationship between poorly formed tumor vasculature and the physiologic characteristics of the cells within the tumor.<sup>[27]</sup> In order to obtain nutrients for their growth and metastatic potential, cancer cells will utilize the host blood vessels, sprout new vessels from existing ones (angiogenesis), and recruit endothelial cells from the bone marrow (postnatal vasculogenesis).<sup>[28]</sup> The anomalous morphology of blood vessels is responsible for the irregular blood flow which results in chaotic blood vessel networks. This interaction between abnormal blood vessels and cancer cells is responsible for the microenvironmental

hallmarks of solid tumors consisting of: low oxygen tension or hypoxia, low extracellular pH or acidosis, and high interstitial fluid pressure. <sup>[19]</sup> The relationship between abnormal blood vessels, hypoxia and is depicted in Figure 1.

**Figure 1: Microenvironment Conditions of the Tumor Present Barriers to Therapy.**

Confocal micrographs from tumor section of human breast cancer xenograft. Blood vessels stained for CD31 (*red*), pericytes for desmin (*green*), and hypoxia for HypoxyProbe™ (*brown*)

a) The tumor microenvironment is typically hypoxic with chaotic vasculature with unstable endothelium, loose pericytes, and leaky vessels. Poor oxygen delivery by the defective vasculature and oxygen consumption by the tumor cells results in hypoxic areas. In addition, the hyperpermeable blood vessels produce a hypertensive extracellular matrix (ECM); Dark brown color represents tissue hypoxia stained with HypoxyProbe.

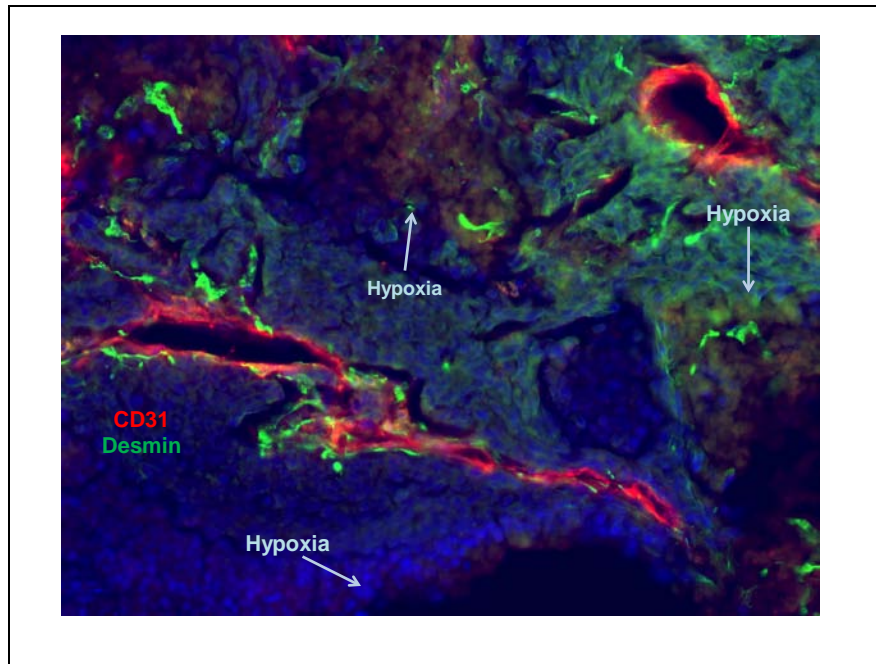
(b) Relationship between abnormal blood vessels and pericytes. Dual immunofluorescence staining for CD31 (*red*) and desmin (*green*) was performed to visualize endothelial cells and pericytes, respectively. The white rectangle shows the process of “sprouting angiogenesis”. Endothelial sprouts tipped by filopodia are abundant on blood vessels and are currently known as a molecular target for the anti-VEGF treatments. Sprouting angiogenesis is characterized by non-mitotic endothelial cell activity, high reversibility, and is always accompanied by pericytes.

**Images were taken by the author of this thesis at the Cancer Biology Department at original magnification x400 and x100 respectively.**

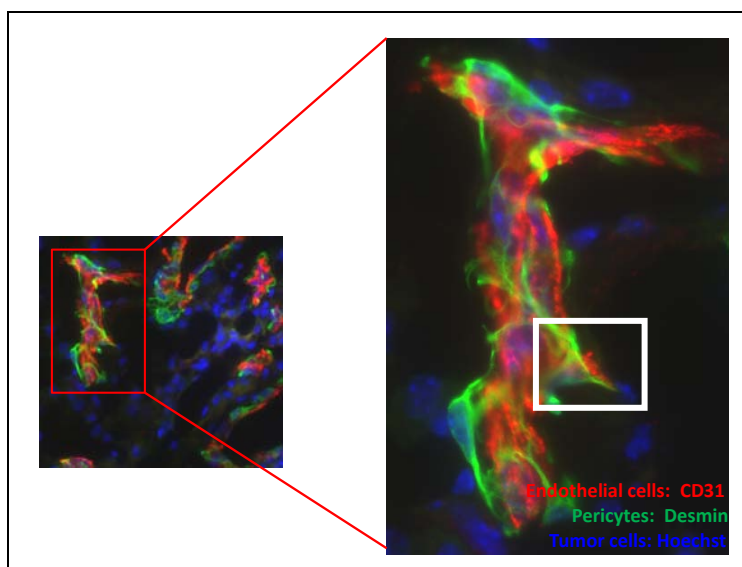


**Figure 1**

- a.** Tumor Microenvironment. Relationship between endothelial cells (*red*), pericytes (*green*) and tissue hypoxia (*dark brown*).



- b.** Tumor Blood Vessels: Endothelial Cells and Pericytes.



These physiological characteristics of tumor microenvironment have been shown to act as an impressive obstacle to the delivery and efficacy of cancer therapy. Novel molecular strategies designed to understand the correct structure and function of tumor vessels and how to interfere with these physiological barriers will improve cancer treatment.

#### **4. Stromal Microenvironment as Cause of Drug Resistance**

In order for an anticancer agent to be therapeutically effective, it should be uniformly distributed through the tumor circulation, cross the vessel wall, and pass through the ECM and finally arrive in the stroma and cancer cells with adequate concentration to cause tumor cell lethality.

Drug resistance remains a principal problem impeding the success of chemotherapy in the treatment of cancer. <sup>[29]</sup> Currently, most of the cancers that are treated with conventional anticancer therapies become resistant to these agents. Two important mechanism of resistance have been identified including intrinsic and acquired resistance. <sup>[18]</sup>

Intrinsic resistance to anticancer drugs, or resistance developed during chemotherapy, remains a major obstacle to successful treatment. In the current literature a large number of published studies about resistance of cancers to chemotherapy focus on cellular and genetic mechanisms as principal factors of resistance, whereas very few describe the role of microenvironment factors. <sup>[30]</sup>

There is a generally accepted hypothesis that tumor cells are genetically unstable and can mutate and that drug resistance of human tumors arises because of the selection of mutant drug-resistant cell during tumor progression, or following exposure to chemotherapy.

This resistance in the clinic manifests itself as lack of initial response –mentioned as refractoriness, or as regrowth after initial response (relapse).

## **Chapter 2**

### **1. Physiological Barriers of Drug Resistance**

The tumor microenvironment possesses several properties that distinguish it from the normal tissues. These differences arise from the irregular characteristics of the blood vessels and the physiologic properties of the cells within the tumor.<sup>[27]</sup> The tumor microenvironment has been recently recognized as a physiological barrier to conventional chemotherapy and radiation-based therapies. These barriers include, tumor hypoxia, tumor acidity (low pH), and high tumor IFP. (Figure 2)

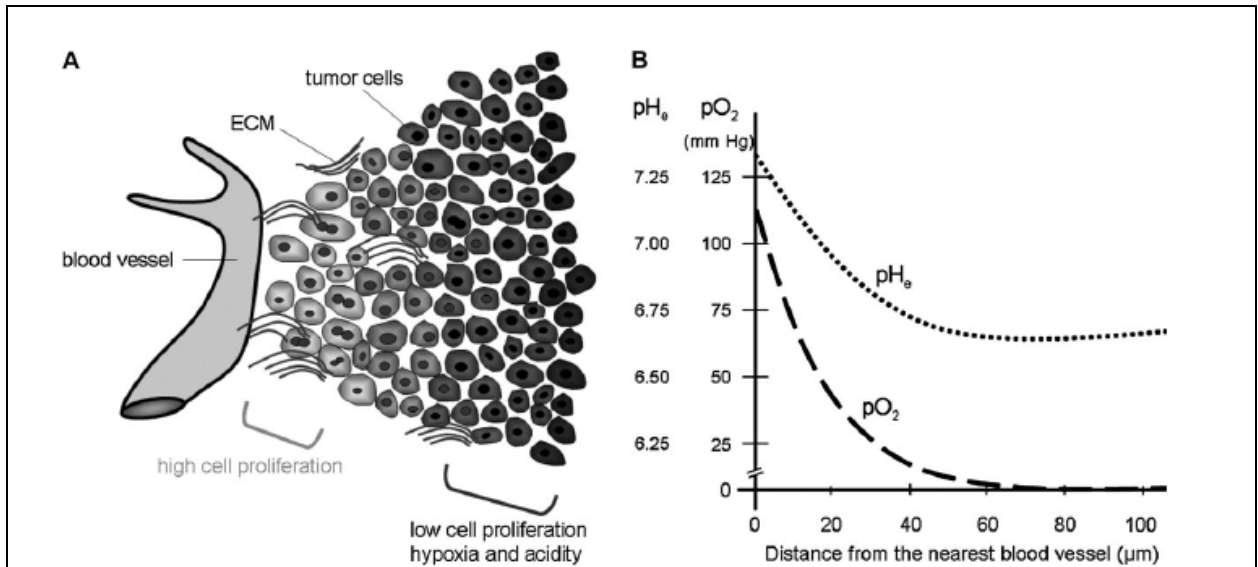
**Figure 2 - Tumor acidosis and Hypoxia**

a) Diagrammatic representation of tumor cells and the extracellular matrix surrounding a capillary.

b) Schematic representation of the gradient of oxygen concentration ( $pO_2$ ; dashed line) and pH (dotted line) in relation to nearest tumor blood vessel.

Graphic obtained with permission from Tedran and collaborators. <sup>[29]</sup>

**Figure 2 - Tumor Acidosis and Hypoxia**



### ***Tumor Hypoxia***

Tumor hypoxia is a universal feature of solid tumors. In contrast to normal tissue, the tumor blood vessels are characterized by the utilization of oxygen which is larger than the oxygen release.<sup>[31, 32]</sup> This imbalance is responsible for inconsistent tissue perfusion, producing high variation of oxygen concentration throughout the tumor mass. Two main causes of tumor hypoxia have been recognized: permanent limitations in oxygen diffusion results in chronic hypoxia, and transient limitations in blood perfusion result in acute hypoxia.<sup>[32]</sup> More importantly, most of the assays of tumor hypoxia currently available do not distinguish between chronic and acute hypoxia. From the clinical point of view, tumor hypoxia has been implicated in the resistance to treatment, especially radiation therapy. In addition, hypoxia is also responsible for malignant phenotype, and is predictive of metastasis and poor outcome in a variety of tumor types.<sup>[33-35]</sup>

Hypoxia-inducible factor-1 (HIF-1) is a transcription factor that regulates multiple genes that are responsible for the adaption of cells to live in normoxia (~21% O<sub>2</sub>) to hypoxia (~1% O<sub>2</sub>) conditions.<sup>[36, 37]</sup> Since the discovery of HIF, more than 2 decades ago, the knowledge of the role of HIF in tumor biology has grown exponentially. Because the broad spectrum of influences of HIF-1, it is actually considered an important target for many tumors. In a very elegant publication, Cairns et al<sup>[38]</sup> using RKO and Su.86 cell lines as preclinical models demonstrated that blocking the HIF-1 pathway represented a novel microenvironment target for solid tumors. In a retrospective review of 150 patients with early invasive breast cancer, treated between 1985 and 1993 in Holland, HIF-1 alpha expression correlated with multiple clinicopathologic variables.<sup>[39]</sup> The results showed that a high level

of HIF-1 alpha was associated independently with shortened disease free survival ( $p = 0.004$ ) and overall survival ( $p = 0.008$ ) in patients with lymph node negative breast cancer.

### ***Tumor Acidosis***

The microenvironment tumor acidosis (pHe) is low compared with the normal tissues. Initially it was thought that the tumor acidosis was the result of accumulation of lactate, the product of anaerobic glycolysis associated with tumor cells. Many of the anti-neoplastic chemotherapy drugs used commonly for cancer treatment are influenced by the microenvironment acidity. In general, the diffusion of drugs into cells occurs by passive diffusion when they are uncharged. However, when drugs are highly polar with acidic or basic groups the cellular uptake depends on the pHe. Thus, basic drugs like doxorubicin, mitoxantrone, and vinblastine have reduced activity in a low pHe due to decreased drug uptake.

In the past, preclinical studies using direct measurement of the pH within tumor models with electrode-based techniques showed that tumor cells can carry out glycolysis and produce lactate are still able to generate an acidic environment. <sup>[40, 41]</sup> Using more modern techniques with <sup>31</sup>P magnetic resonance spectroscopy to measure the characteristics of pH-dependent microenvironment in solid tumors, it was determined that the acidity within the tumor is a combination of the pHe and the internal, intracellular pH (pHi). Cells within the tumor are capable of maintaining a reasonably neutral cytosolic pH in the face of external acidosis. <sup>[42]</sup>



## Chapter 3

### 1. Interstitial Fluid Pressure and Transvascular Transport

#### *The interstitium*

New strategies to improve the distribution of drugs between normal and tumor tissues that reduce toxicities associated with chemotherapy regimens for solid tumors in conjunction with increase efficacy are warranted. A potential target is tumor IFP.

The ECM or interstitium consists of the collective spaces between cells, and accounts for approximately one sixth of the total body volume.<sup>[43]</sup> The extracellular compartment is composed of a collagen fiber scaffold that contains a gel phase made up of hyaluronan, glycosaminoglycans (GAGs), salts, and plasma-derived proteins.<sup>[43]</sup> The collagen structure is thought to physically restrain the intrinsic tendency of the hyaluronan and the glycosaminoglycans to swell, thus reaching equilibrium.<sup>[44, 45]</sup>

Interstitial fluid, made up of water and solutes, acts as the transport medium for the exchange of nutrients, waste products, and oxygen. IFP is the result of oncotic pressure in the interstitial space, oncotic and hydrostatic pressures in the microvascular space, the reflection coefficient, and the hydraulic conductivity of the vascular wall and interstitial space. Together these forces determine the net filtration pressure across the capillary plasma membrane and are determined by the Starling equation:<sup>[46]</sup>

$$J_v = K_f [(P_c - P_{if}) - \sigma(COP_c - COP_{if})],$$

Where fluid transport across the capillary wall can be described quantitatively,  $J_v$  is net capillary fluid filtration,  $K_f$  is the capillary filtration coefficient,  $P_c$  and  $P_{if}$  are the hydrostatic

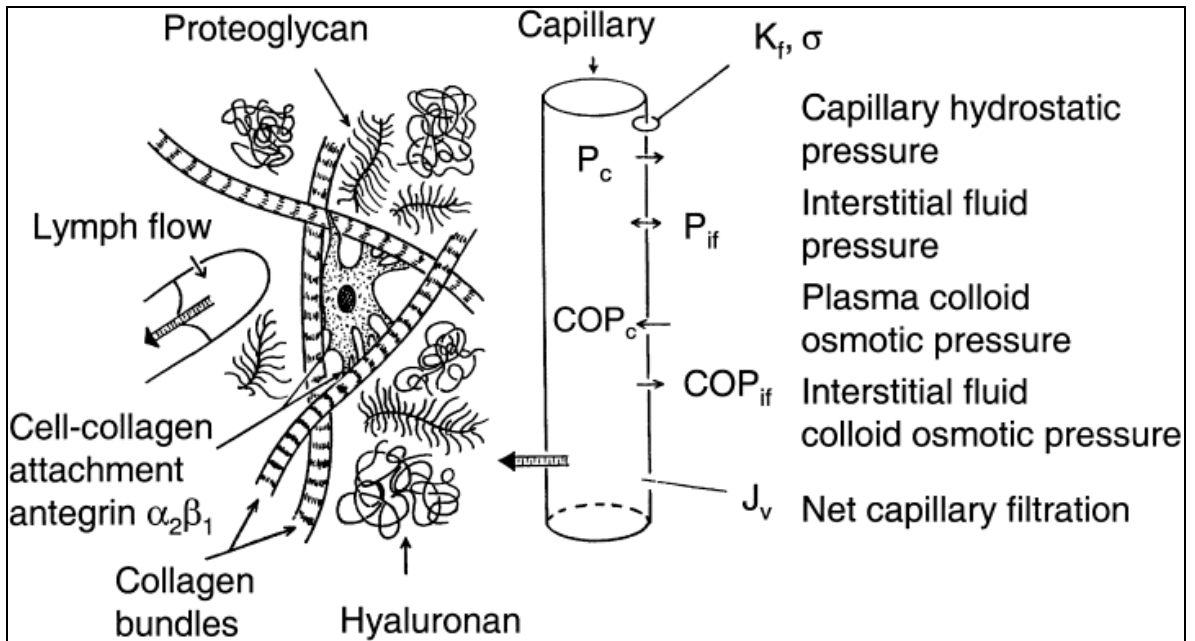
pressures in capillary and interstitium, respectively,  $COP_c$  and  $COP_{if}$  are the corresponding colloid osmotic pressures, and  $\sigma$  is the capillary reflection coefficient for proteins.

This traditional concept of transcapillary fluid flux is the product of the pressure imbalance across the capillary wall, and does not include cells in the regulation of interstitium. A new concept in the interstitium fluid regulation included connective tissue cells that are not organ specific but are an integral part of the extracellular matrix. (Figure 3)

**Figure 3:** Overview of the transcapillary-interstitial fluid exchange system.

The transcapillary hydrostatic (P) and colloid osmotic pressure (COP) determines capillary fluid flux. Subscripts “c” and “if” denote plasma and capillary reflection coefficient, respectively. The capillary net filtration pressure is normally 0.5 to 1 mmHg and results in a net fluid filtration ( $J_v$ ) that is removed by lymph flow. Collagen and hyaluronan are abundant structural component of loose connective tissues. Graphic obtained with permission from Wiig and collaborators. <sup>[45]</sup>

**Figure 3 - Overview of the transcapillary-interstitial fluid exchange system**



### ***Regulation of the IFP***

The normal tissues possess a very sensitive regulation of ECM fluid. For instance, in most tissues of the body, the IFP under normal conditions is slightly negative, e.g. about -1 mmHg in the skin. However, under pathological conditions, such as burn injuries, urticaria or inflammation, the net filtration pressure increases tremendously due to a fall in the IFP to as low as -150 mmHg, resulting in edema formation.<sup>[47]</sup> This example illustrates that there is also an active control of the transcapillary exchange of fluids by the interstitium. Moreover, it also implies that cells in the interstitial compartment, e.g. fibroblasts, and pericytes are important regulators of the IFP. One possibility for the cells in the connective tissues to exert a controlling force over the IFP is via the contacts made between the cell and ECM constituents through integrins.<sup>[44]</sup> Another possibility is related to the mesodermal origin of such cells and the contraction capacity eliciting changes in the ECM.

### ***IFP is Elevated in Solid Tumors***

The clinical measurement of IFP in normal subcutaneous tissues and muscle tissues show a range from -2 to 4 mm Hg.<sup>[48, 49]</sup> In contrast, solid tumors have elevated IFP compared with normal tissue, with a steep rise in pressure starting at the periphery of the tumor. Interstitial pressure was first noted to be elevated in animal tumors in 1950 by Young and colleagues,<sup>[50]</sup> and the first data on interstitial tumor pressure in humans were published in 1990.<sup>[51, 52]</sup> These studies suggest that many human tumor nodules have interstitial pressures much greater than in normal tissues. The precise cause of increased tumor IFP is not well understood: a number of mechanisms have been hypothesized, yet none experimentally confirmed. Explanations included scarcity of lymphatic vessels, tumor fibrosis, and the leaky nature of tumor vessels, caused by an increased signaling from vascular endothelial growth

factor receptor. <sup>[53]</sup> Implantation of the same tumor cell line at diverse sites in mice produces dissimilar IFPs, suggesting that the microenvironment impacts tumor IFP. <sup>[54]</sup> Nowadays, we accept that the cause of high tumor IFP is multifactorial.

### ***Consequences of Elevated IFP***

Elevated IFP in tumors is a consequence of severe microvascular, lymphatic, and interstitial abnormalities. In accordance with an increased IFP, the oncotic pressure of tumor interstitial fluid is also elevated compared to normal tissue and is close to that of plasma, indicating that there is a reduced transport of fluids into tumors compared with normal tissues. <sup>[55]</sup> This could affect the distribution of therapeutic antibodies into tumors because macromolecules are thought to be transported preferentially through convection. However, a high tumor IFP could also conceivably hinder the delivery of low molecular weight compounds, which are thought to be transported mainly by diffusion in normal tissue. The microvascular exchange barrier in tumors is nonselective, because of its leaky nature, and thereby favors convective transport of water-soluble low molecular weight agents. Also, the increased water content in tumors may facilitate diffusion of molecules through the tumor interstitium. <sup>[56]</sup> Indeed, studies in experimental models have shown that lowering tumor IFP, either by pharmacologic interference or by increasing the transcapillary hydrostatic pressure gradient, is paralleled by an increased transport of both macromolecules and low molecular weight compounds. <sup>[56, 57]</sup> Local delivery of prostaglandin E1 to tumors in rats lowered the IFP and enhanced the penetration of <sup>51</sup>Cr-EDTA. <sup>[56]</sup> Targeted delivery of tumor necrosis factor- $\alpha$  to tumor vessels in mice enhanced the penetration of doxorubicin into tumors. <sup>[57]</sup>

In a series of patients with cervical carcinoma there was a correlation between interstitial pressure and the oxygenation status of the tumor and an inverse correlation with tumor response to radiation therapy.<sup>[58]</sup> In another study in patients with cervical cancer, tumor IFP was a strongly independent prognostic marker for radiation therapy of cervical cancer.<sup>[59]</sup> In this study, 102 eligible patients with locally advanced cervical cancer were evaluated during treatment with radiation therapy. The IFP assessment was done using a wick-in-needle technique. Patients with high IFP were more likely to recur both locally and at distant sites. In addition, patients with high IFP were significantly more likely than those with low IFP to recur after radiotherapy and die of progressive disease.

#### ***Role of Platelet-Derived Growth Factor Receptor in tumor IFP Regulation***

Platelet-derived growth factor (PDGF) is a mitogen and a chemoattractant for cells of mesenchymal origin, e.g. fibroblasts and smooth muscle cells, which acts by binding two structurally related tyrosine kinase receptors. Different roles in the paracrine stimulation of tumor stroma have been described for PDGF.<sup>[60]</sup>

The well-documented PDGF  $\beta$ -receptor expression in the stromal compartment in many common solid tumors (lung, breast, colon), which also are characterized by tumor interstitial hypertension, is consistent with a role of PDGF  $\beta$ -receptors in the control of tumor IFP.<sup>[61]</sup> The tyrosine kinase inhibitor imatinib inhibits the kinase activities of the PDGF receptors, c-Kit, ABL, and ARG with similar potencies.<sup>[62]</sup> Imatinib –a potent inhibitor of BCR/ABL oncoprotein and c-Kit receptor- is currently used in the treatment of chronic myelogenous leukemia and gastrointestinal stromal tumors. Three preclinical studies have examined the effect of imatinib on the IFP in experimental tumor models,<sup>[63-65]</sup> and analyzed

in a separate publication. <sup>[66]</sup> The first of these studies found that rats with colonic carcinomas treated with imatinib exhibited a reduced IFP measured by the wick-in-needle technique. Treated tumors showed a mean IFP of 11.3 +/- 1.1 mm Hg, whereas untreated tumors displayed a mean IFP of 16.8 +/- 0.9 mm Hg ( $p < 0.01$ ). Subsequently treatment with imatinib increased the uptake of freely diffusible tracer <sup>51</sup>Cr-EDTA into the tumors ( $p < 0.05$ ) compared with untreated animals. <sup>[63]</sup> The second study in mice showed that imatinib induced lowering of IFP was paralleled by an enhanced tumor content of paclitaxel. <sup>[64]</sup> Mice with KAT-4 tumors were injected with [<sup>3</sup>H] paclitaxel and radioactivity was measured 8 or 24 hours. Mice treated with imatinib significantly increased tumor uptake of [<sup>3</sup>H] paclitaxel compared with the control group ( $p < 0.05$ ). Imatinib had no direct effect on tumor growth, but the combination of imatinib and paclitaxel, increased the efficacy of chemotherapy. In the third study, mice injected with human thyroid carcinomas were treated with various doses of the epothilone B (EPO906 or patupilone a novel anti-microtubular agent), alone or in combination with imatinib. <sup>[65]</sup> The combination was more effective than chemotherapy alone, and tumors treated with the combination were more than 40% smaller. In addition, there was a tumor-specific, three-fold increase in tumor level of EPO906. Interestingly, various treatment regimens of imatinib showed a correlation between the ability of the treatment to lower tumor IFP and enhanced tumor uptake and efficacy of EPO906.

These studies clearly establish that inhibition of PDGF receptor signaling is a novel strategy for enhancement of chemotherapeutic effects on solid tumors. These data also suggest that the reduction of tumor IFP is related to the drug uptake and is one of the



mechanisms of tumor sensitivity. There are currently several clinical trials in advanced solid tumors, exploring the combination of standard chemotherapy with imatinib.

### ***IFP and transvascular transport in tumors***

Extravasation of materials from the blood vessels can occur by diffusion and convection and is described by the following equation:<sup>[67]</sup>

$$J = PS (C_p - C_i) + L_p S (1 - \sigma) [(P_v - p_i) - \sigma (\pi_v - \pi_i)] C_p$$

$J$  is the flux (mass per unit volume) of materials crossing the vessel wall,  $P$  is the vascular permeability,  $S$  is the vessels' surface area,  $C_p - C_i$  is the concentration difference of the material between the plasma and the interstitial space,  $L_p$  is the hydraulic conductivity of the vessel wall,  $P_v - p_i$  is the difference between microvascular and IFP,  $\sigma$  is the osmotic reflection coefficient, and  $\pi_v - \pi_i$  is the osmotic pressure difference across the wall. The vascular permeability depends on the properties of the particle (size, charge and configuration) and the vessel wall (pore size, charge and arrangement). It decreases as the particle size increases and becomes zero when the particle size is larger than the pore cut-off size. The hydraulic conductivity is a property of the morphology of the wall surface occupied by pores.

Young and collaborators, showing that the “tissue pressure” of testicular tumors is substantially higher than in normal tissue, did the first preclinical tumor IFP assessment.<sup>[50]</sup> Since then, multiple other investigators have demonstrated that the IFP of most, if not all, experimental and clinical tumors is elevated.<sup>[68]</sup> During the last four decades multiple investigators have measured tumor IFP in several tumor types. For instance, pressures of up

to 60 mmHg were found in melanomas <sup>[69-71]</sup> and the mean IFP of head and neck carcinomas was shown in a large number of patients to be 19 mmHg. <sup>[52]</sup> Still, the etiology of tumor IFP is unclear, the tumor microvascular pressure has been found to correlate with the IFP. <sup>[69]</sup> This evidence support the concept that the stromal compartment is likely to be an important determinant of tumor IFP, since implantation of the same tumor cell line at diverse sites gives rise to dissimilar absolute pressures. <sup>[54]</sup>

One of the consequences of the high IFP in tumor tissue has been proposed to be an impaired transvascular transport of fluids and molecules into the tumor interstitium. <sup>[60]</sup> Several investigators demonstrated that the tumor interstitium has unique biophysical properties provide experimental support for this proposal. <sup>[72, 73]</sup>

Many investigators have used pharmacological intervention to lower the tumor IFP as a viable strategy to increase the uptake of anti-cancer drugs into tumors, thereby achieving higher quantities of effective treatment into the tumor. Several agents administered either locally or systemically, have been shown to alleviate the interstitial hypertension in the experimental setting. Various substances, such as nicotinamide and a bradykinin B2 agonist, act on the microvasculature, whereas others, such as hyaluronidase, affect the microenvironment. It is notable, however, that the precise mechanism of action in most treatments is not well understood.

### ***Tumor Angiogenesis and Interstitial Hypertension***

The growth of neoplastic cells in a confined and stiff interstitial matrix can induce solid stress, causing an increase in microvascular pressure (MVP) and IFP. The MVP is dependent on arteriovenous pressure differences and the geometric and viscous resistance to blood

flows. Boucher, et al, hypothesized that MVP is a major determinant of IFP due to the high permeability of tumor vessel and the lack of functional lymphatics.<sup>[69, 74]</sup> The same group of investigators<sup>[75]</sup> reported that taxanes inhibit the growth of murine mammary carcinoma (MCA-IV) and the human soft tissue sarcoma (HSTS-26T). After treatment with paclitaxel blood vessels were measured at 48 and 96 hours, demonstrating that the diameter increased significantly. The increase of vascular diameter was associated with reductions in MVP and IFP. Thus, taxanes might be responsible for the increase of delivery of therapeutic agents into the tumor.<sup>[76]</sup>

VEGF is a potent angiogenic factor released by a variety of normal and neoplastic cells following a hypoxic stimulus. VEGF was originally discovered as a vascular permeability factor (VPF) a glycoprotein secreted by tumor cells that potently stimulates ascites formation and vascular leak.<sup>[77]</sup> This vascular leak, most probably contributes to the elevated interstitial pressure of ECM commonly seen in solid tumors. A recent report showed that blocking the VEGF signaling by a VEGF-receptor-2 antibody decreases the IFP in a variety of tumor models, not by restoring the lymphatic function, but by producing a morphologically and functionally normalized vascular network.<sup>[78]</sup> The same investigators also report that an anti-VEGF antibody can lower IFP in rectal carcinomas in patients.<sup>[79]</sup> Thus, this process of “vascular normalization” might be responsible for the increase of survival rates in animal studies and for the efficacy demonstrated with patients with rectal cancer after treatment with combination of bevacizumab and cytotoxic chemotherapy.

One of the main functions of pericytes consists in providing stability of blood vessels. It is also critical in the development of microvessels in many organs. Pericytes –as well as

endothelial cells, are also sensitive to anti-VEGF treatments. A recent study demonstrated that pericyte density is affected by anti-VEGF therapies.<sup>[80]</sup> Therapeutic benefits were recently observed after combination of the VEGF antagonist with imatinib in a genetic model of insulinomas, presumably through imatinib-mediated targeting of PDGF receptors on pericytes.<sup>[81]</sup> This study also provided evidence of the important role of PDGF-BB and PDGF-DD in pericyte recruitment to tumors. Together, these observations suggest that pericytes represent an important target for the anti-VEGF treatment.

## **Chapter 4**

### **Investigation of Tumor IFP in a Xenograft Breast Cancer Model**

The fact that most solid tumors possess a high interstitial tumor pressure, led us to propose that tumor hypertension can be responsible for the tumor drug uptake which might be responsible of tumor efficacy. Using a xenograft tumor model, we set out to investigate the effect of tumor IFP using two doses of paclitaxel and bevacizumab, analyzing the efficacy of the combination of anticancer drugs and transvascular drug transport.

## Material and Methods

### *Cell Line*

Dr. Janet E. Price provided the GILM2 cell line. This cell line was originated from GI101A human breast cancer cell line initially provided by Goodwin Institute for Cancer Research, Inc. (Plantation, Florida) <sup>[82]</sup> Lung metastasis-derived lines were established as follows; the lung from mice injected with GI101A cells were minced finely and plated in culture dishes. The resulting culture was named GILM1. This cell line was expanded in culture and injected into mice. Metastases in the lungs of these animals were isolated and the procedure repeated to produce the line GILM2 (a pool from the metastases of three mice). <sup>[83]</sup> This new cell line demonstrated a higher anchorage-independent growth, tumorigenicity and spontaneous lung metastasis than GI101A cells. <sup>[84]</sup>

For the experiments *in vitro*, we seeded  $2 \times 10^6$  cells/ml and cells were maintained in monolayer culture in Dulbecco's minimum essential medium-F12 medium (DMEM/F12) supplemented with 10% FBS, L-glutamine, 5% v/v insulin-selenium-transferrin supplement (Sigma Chemical Co., St Louis, Missouri). Actual cell numbers were calculated by multiplying diluted times compared with initial cell numbers. Cell viability % = viable cell numbers/total (viable + dead) cells numbers x 100%. Inhibition % = (control groups-experimental groups)/control groups for viable cell numbers x 100%. Differentiation was evaluated by nitroblue tetrazolium (NBT, Sigma) reduction test.

To determine the *in vitro* tumor growth inhibition of GILM2 cells by the reagents, cells were cultured in monolayer culture. GILM2 cells were plated in 96-well culture plates at an initial density of  $5 \times 10^3$  cells per well, and allowed to attach for 24 h. The culture

medium was then changed and the cells were incubated for a further 72 hr in different culture conditions: medium alone, with paclitaxel (1 - 10 nM), with bevacizumab (0.1 - 10 ug/ml) or a combination of these agents. Relative cell numbers were determined using MTT. Aliquots of 40 ul of a 5 ug/ml solution of MTT were added to each well and incubated for 2hr; the medium was then aspirated and the cells lysed by the addition of 100 ul DMSO. The conversion of MTT to formazan in metabolically viable cells was monitored with a MR-5000 microtiter plate reader to read at 570 nm (Dynatech, Inc Chantilly, VA). All assays were performed in triplicate, with a minimum of three independent experiments.

### *Animals*

Female athymic NCr-nu mice were purchased from the NCI-Frederick Cancer Research Facility (Frederick, Maryland). The mice were housed in a specific pathogen-free facility and used at seven to eight weeks of age. The care and use of laboratory animals were in accordance with the principles and standards set forth in the Principles for Use of Animals (NIH Guide for Grants and Contracts), the Guide for the Care and Use of laboratory animals and the provisions of the Animal Welfare Acts. The ACUF Protocol (#11-07-12731) was approved on November 21, 2007.

### *Reagents*

Paclitaxel (Taxol®, Bristol Myers Squibb) was obtained from the MD Anderson Cancer Center central pharmacy. It was stored at room temperature and diluted with phosphate buffered saline (PBS). Two doses of paclitaxel were defined: low dose (LD) 15 mg/kg twice

a week, and high dose (HD) 24 mg/kg twice a week. Bevacizumab (Avastin®, Genentech) was obtained from the MD Anderson Cancer Center central pharmacy and was stored at 4°C. Two doses of bevacizumab were defined: low dose (LD) 5 mg/kg twice a week, and high dose (HD) 10 mg/kg twice a week. Both experiments were conducted separately.

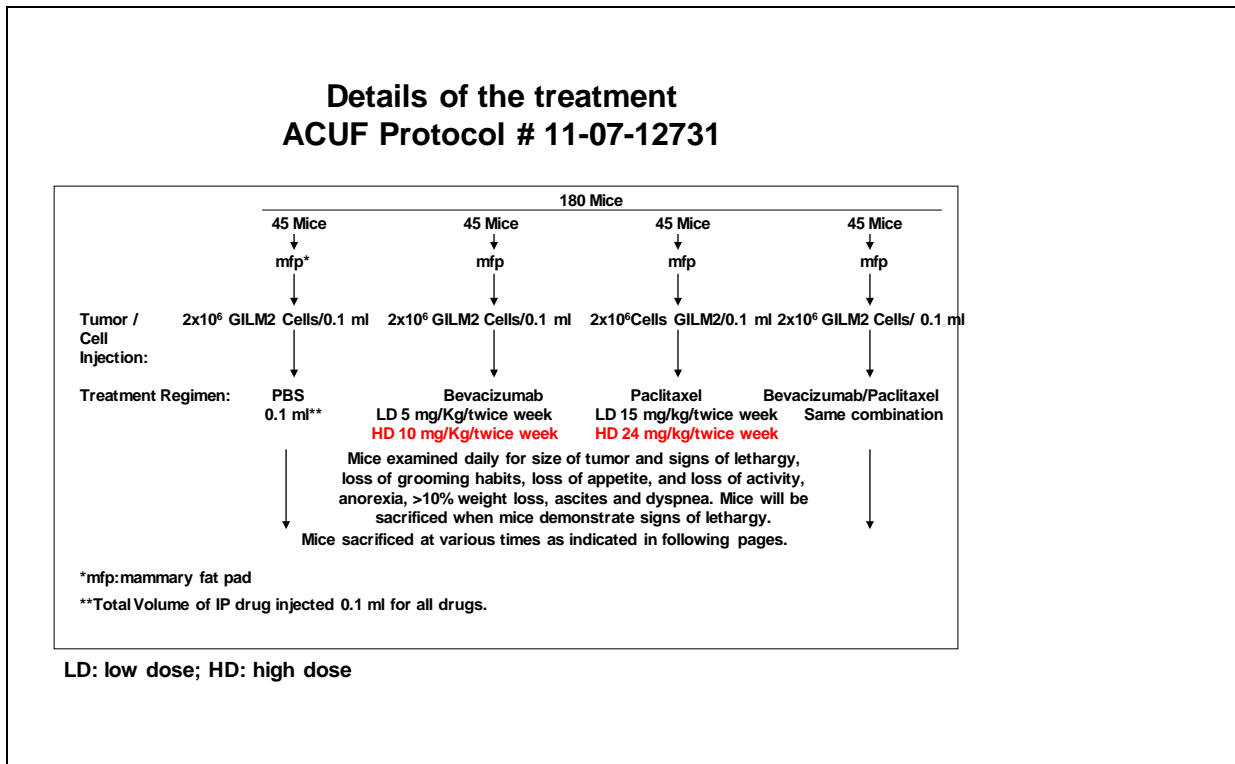
In the LD experiment mice were randomized into four groups (n=10/group) and the following treatments were initiated: (a) vehicle control (PBS i.p. injection twice a week), (b) paclitaxel (15 mg/kg i.p. injection twice a week), (c) bevacizumab (5 mg/kg i.p. injection twice a week, and (d) the combination of paclitaxel and bevacizumab (same doses, i.p. injection twice a week).

In the HD experiment mice were randomized into four groups (n=10/group) and the following treatments were initiated: (a) vehicle control (PBS i.p. injection twice a week), (b) paclitaxel (24 mg/kg i.p. injection twice a week), (c) bevacizumab (10 mg/kg i.p. injection twice a week, and (d) the combination of paclitaxel and bevacizumab (same doses, i.p. injection twice a week). Following 3 weeks of therapy, mice were sacrificed. Body weights were recorded, and tumors were weighed and collected.

The description of the treatment is depicted in Figure 4.



**Figure 4 - Description of the Experimental Treatment**



### *Tumor Growth*

For all *in vivo* experiments, tumor cells in exponential growth phase were harvested by brief exposure to 0.25% trypsin in 0.02% EDTA, then washed and resuspended in  $\text{Ca}^{2+}$  and  $\text{Mg}^{2+}$  free PBS, to give a dose of  $2.5 \times 10^6$  cells in 100 $\mu\text{l}$ . This dose of cells was injected into the mammary fat pad (mfp) of mice. Local tumor growth was measured at two weekly intervals, using calipers, recording two perpendicular diameters to calculate the mean tumor diameter.

Tumors were established by implantation of human breast cancer cell line GILM2 (dose  $2 \times 10^6$  cells/0.1 ml) into mammary fat pad (mfp) in 5 – 6 weeks old female mice. Mice were monitored twice a week for tumor growth, and experiments were performed on week 4-5 after injection on mice bearing tumors ranging in size between 0.5  $\text{cm}^3$  and 1  $\text{cm}^3$ .

Mice were kept under specific pathogen-free condition. Sterilized food and tap water were given *ad libitum*. Drug efficacy was assessed in terms of tumor volume and body weight, and was recorded three times a week. Tumor volume were calculated as  $V = a^2 \times b \times \pi/6$ , where  $a$  and  $b$  equal the short and the long diameter of the tumor, respectively. Once tumors became median size of 500  $\text{mm}^3$ , approximately at day 45 of the experiment, mice were treated with i.p. injection of paclitaxel and bevacizumab twice a week. Measured tumor of 1.5 cm mean diameter were either surgically removed and the incision closed with wound clips, or the mouse was euthanized. All mice were necropsied, and tumors removed for culture and/or histopathological analysis after three weeks of treatment. All *in vivo* experiments were conducted in accordance with the guidelines of the MD Anderson Cancer Center Animal Care and Committee.

#### *Interstitial Fluid Pressure Measurement.*

Tumor IFP was measured using the ultraminiature tipped catheter described by Dr. Ozerdem.

<sup>[85]</sup> Following general anesthesia with isoflurane (1.5%-2.5% isoflurane delivered at 1-2 L/min) ultraminiature transducer-tipped catheter in which the sensor is side-mounted at the tip: SPC-320 transducer (2 French in size, 0.66 mm in diameter) and the ultraminiature pressure transducer were introduced into the tumor protected with 18-gauge needle to the core of the tumor. The Mikro-Tip (PSC-320 Millar) was connected to transducer Millar. The transducer was connected to a PowerLab 8/30 amplifier and the data was imported into software to a Macintosh computer. Records of tumor IFP were done in mm Hg. The needle was removed slowly while the sensor was introduced into the center of the tumor. The location of the center of the tumor is estimated by dividing the caliper-measured diameter of tumor in half. This procedure was performed at baseline and then twice per week. Each measurement lasted approximately 3 to 5 minutes. The tumor measurement equipment is depicted in Figure 5.

**Figure 5** - Equipment to assess the IFP with ultraminiature pressure transducer.

A. The ultraminiature transducer (arrow) is introduced percutaneously into a surface of the tumor in a protective metal guide (18-gauge needle) (arrowhead).

B. The needle is withdrawn slowly, while the sensor is introduced into the center of the tumor. The location of the center of the tumor is estimated by dividing the caliper-measured diameter of tumor in half. The transducer can be marked for millimeter gradation using standard fine point pens.

C. Handling of the needle guide and transducer is very easy during microsurgical procedures on mice. Scale bar = 600  $\mu\text{m}$ . Pictures A, B, and C were obtained from Ozerdem and Hargens. <sup>[85]</sup>

D. Millar catheter introduced into the 18-gauge needle. F. Mac Laptop, connected to PowerLab 8/30 amplifier and the data was imported into software to a Macintosh computer.

**Figure 5:** Interstitial fluid pressure measurement with ultraminiature pressure transducer.



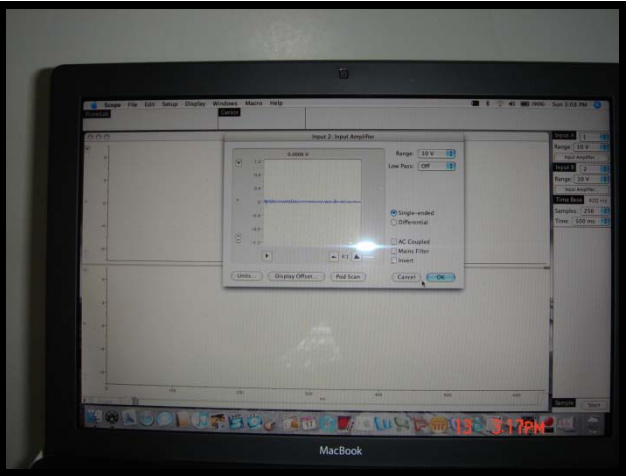
**D**



**E**



**F**



### *Immunohistochemistry Analysis*

Tumor tissue was fixed in 10% buffered formalin for paraffin embedding, or frozen in OCT compound (Miles Laboratories, Elkhart, Indiana) in liquid nitrogen. For assessment of blood vessel quantification, 5µm frozen tissue sections were cut, fixed in acetone and stained with antibodies to CD31/PECAM-1 (PharMingen, Sand Diego, California) with fluorescent Alexa 647 antirat secondary antibody (Invitrogen). This experiment has been described elsewhere.<sup>[86]</sup> Non-specific IgG was used for control reactions. Areas of sections with the highest numbers of stained capillaries and small venules were identified by scanning the sections at low power magnification (40X). Images of 10 fields at higher magnification (100X) from these selected areas were captured using a digital camera and stored for analysis.

ImageJ software (National Institute of Health) was used to assess vessel area, vessel diameter, and length. Vessel area was calculated from number of pixels stained with CD31 per high-power field. Vessels diameter and length were calculated from measuring pixels of each vessel at its largest diameter or length and converting pixels to micrometers. Sections were counterstained with hematoxylin. The CD31 and pericyte staining, area was quantified (40X objective, 20 fields from each slide) by using ImageJ software (National Institute of Health).

Sections of paraffin-embedded tumor that had been formalin-fixed were used to identify cleaved-caspase 3. Immunohistochemistry using the rabbit anti-cleaved caspase 3 antibody was performed on deparaffinized tissue sections using a routine avidin-biotin-immunoperoxidase technique [Vectasin Elite avidin-biotin-immunoperoxidase kit reagents (Vector Labs, Burlingame, CA)]. Before incubation with the primary antibody (1:200

dilution as supplied by the manufacturer), tissue sections were subjected to heat-induced epitope retrieval by incubation in a Ph 8.0 0.01 M EDTA solution for 10 min in a vegetable steamer, followed by 20-min cool-down and treatment with 3% hydrogen peroxide before antibody application. Microscopy: fluorescence images were prepared using a Zeiss Axioplan 2 microscope equipped with phase-contrast optics and with rhodamine and UV channel filters. Images were recorded using either a Dage 300 monochrome CCD camera or a Zeiss AxioCam CCD camera, and composite figures were prepared using Adobe Photoshop.

#### *Immunofluorescence double staining for CD31 and Desmin*

Sections were fixed in cold acetone for 10 min, blocked with protein blocker for 20 min at room temperature, incubated with CD31 antibody (1:400; PD PharMingen) overnight at 4°C followed by incubation with Alexa Fluor 594-conjugated with anti-rat antibody (1:1,000; Invitrogen) for 1 hour at room temperature. After washing with PBS, samples were incubated with desmin antibody (1:400; DakoCytomation) for 1 hour and followed by incubation with Alexa Fluor 488-conjugated anti-rabbit antibody (1:1,200; Invitrogen) for 1 hour at room temperature. Samples were counterstained with Hoechst for 5 min and mounted.

#### *Hypoxia Measurement*

Pimonidazole hydrochloride (HypoxyProbe<sup>TM</sup>, 100 mg/kg/0.2 ml PBS) was administered IP to tumor-bearing mice and this agent is metabolized and bound to hypoxic cells within the tumor.<sup>[87]</sup> Three hours after injection, tumors were excised and frozen in liquid nitrogen. Frozen sections (10µm thick) from the central regions of tumors were fixed for 15 min in 4%

FBS, 5% nonfat milk, and 0.1% Triton X-100 in PBS. Slides were incubated for 1 hour at room temperature with an FITC-conjugated monoclonal antibody against pimonidazole (1:20) (Millipore) and counterstained with 50 nM propidium iodine (PI). FITC and PI fluorescent signals for entire tumor sections (one section per tumor) were acquired on a Nikon Eclipse E800 microscope equipped with motorized scanning stage, a 12-bit QImaging camera (QImaging, Burnaby, Canada)

#### *Lectin Perfusion and Tumor Vascular Staining.*

Mice were anesthetized and injected intravenously (tail vein injection) with 100 µl of fluorescein *Lycopersicon esculentum* lectin (Vector Laboratories). Ten minutes later, we perfused mice through the ascending aorta with 4% paraformaldehyde for 2 minutes. Tumors were extracted, placed in 4% paraformaldehyde for another 2 hours followed by immersion in 30% sucrose/PBS overnight. Tumor samples were then embedded in OCT, and cryostat sectioned for visualization using confocal fluorescence microscopy.

#### *Intratumoral Drug Distribution of Labeled-Paclitaxel*

In this aim, we aimed to investigate the influence of bevacizumab on the antitumor activity of paclitaxel and the intratumoral distribution in GILM2 model. This aim was conducted under the guidance of Dr. William G. Bornmann, Professor of Experimental Therapeutics. Thirty mg of paclitaxel were conjugated to Dansyl dye. Reconstitution was done in DMSO following by i.p. injection of 24 mg/kg of labeled-paclitaxel. Dansyl chloride or 5-(dimethylamino) naphthalene-1-sulfonyl chloride is a reagent that reacts with primary amino



groups in both aliphatic and aromatic amines to produce stable blue- or blue-green-fluorescent sulfonamide adducts. The absorption value was always taken at the maximum that appears between 310 nm and 350 nm. The conjugations of dansyl chloride with paclitaxel in the tumor possess a dark blue color.

*Determination of Transcapillary Transport of Paclitaxel into the Tumor Tissue Using Liquid Chromatography/Mass Spectrometry (LC/MS)*

LC/MS is a simple, rapid and sensitive analytical method for quantifying paclitaxel in tissue homogenates.<sup>[88]</sup> This aim was conducted under the guidance of Dr. Timothy L. Madden, Director of the Pharmacology and Analytical Facility. This method combines a one-step liquid-liquid sample extraction with ESI  $\pm$  MS/MS detection to achieve the selective and specific quantization of paclitaxel. The assay has been fully validated by previous preclinical studies at MD Anderson Cancer Center.<sup>[89, 90]</sup>

**Statistical Analysis**

All experiments were repeated at least two times on different occasions. The results are presented as the mean  $\pm$  95% confidence intervals for all values. All data were analyzed using GraphPad Prism 4 (GraphPad Software, Inc) and the Mann-Whitney nonparametric *t* test. A *p* value of <0.05 was considered statistically significant.

## **Results**

The experiment aims and the diagram of treatment plan is depicted in Figure 6.

**Figure 6**

## Flow Sheet of the Treatment

IFP\*: During the first week of experiment a total of 3 measurements, and during the 2<sup>nd</sup> and 3<sup>rd</sup> weeks one measurement each week.

Perfusion study: During the first week of the experiment a total of 2 assays, and during the 2<sup>nd</sup> and 3<sup>rd</sup> weeks one assay each week.

Hypoxia study: During the first week of the experiment a total of 2 assays, and during the 2<sup>nd</sup> and 3<sup>rd</sup> weeks once each week.

Tumor Volume measurement: two times a week.

Diagram of Treatment Plan:

Days/ Drug	1	2	3	4	5	6	7	8	9	10	11	12	13	14	15	16	17	18	19	20	21	22
PBS		x				x			x				x			x				x		
Bev	x					x			x				x			x				x		
Pac			x			x				x			x				x			x		
Bev/ Pac		x	x			xx			x	x			xx			x	x			xx		

•IFP:	↑					↑							↑							↑		
• Perfusion	↑(4)							↑(3 per arm)					↑(3 per arm)							↑(3 per arm)		
• HypoxyProbe	↑(4)							↑(3 per arm)					↑(3 per arm)							↑(3 per arm)		
• Paclitaxel	↑(4)							↑(3 per 2 arms)					↑(3 per 2 arms)							↑(3 per 2 arms)		
Assay																						
• IHC	↑(4)							↑(3 per arm)					↑(3 per arm)							↑(3 per arm)		
Sacrificed mice: 16								42					42							42		
Remaining alive:164								122					80							38		

IFP\*:Interstitial Fluid Pressure; IHC: Immunohistochemistry

### *In vitro* treatment of culture cells using paclitaxel and bevacizumab

The GILM2 breast cancer human cell line was used for this experiment. The cells were determined to be free of mycoplasma and 17 different murine viral pathogen before use.

#### *Clonogenic Assay*

The combination of paclitaxel plus bevacizumab and paclitaxel as single agent results in no visible colonies. (Figure 7 a) The bevacizumab and control dishes have colonies in the same proportion. The interpretation of this experiment is that the GILM2 breast cancer cells are sensitive to paclitaxel, and insensitive to bevacizumab. One conclusion of this experiment is the absence of bevacizumab sensitivity response might be mediated by the lack of VEGF receptors in the tumor cell.

#### *MTT Assay*

We performed a 3-(4,5-dimethylthiazol-2-yl)-2,5-dephenyltetrazolium bromide (MTT) to correlate with the clonogenic assay performed. Several serial dilutions of bevacizumab and paclitaxel plus bevacizumab were performed and we found similar results to those of the clonogenic assay. The plots in Figure 7 b, demonstrated that GILM2 is insensitive to increasing doses of bevacizumab as single agent as well in combination with paclitaxel. GILM2 cells are sensitive to paclitaxel. Increasing paclitaxel doses produced a dose response curve.

## **Figure 7**

**a.** Clonogenic assay performed in 4 Petri dishes, with GILM2  $1 \times 10^2$  breast cancer cells. The control group was treated with PBS only, the paclitaxel flask was treated with 5 nM of paclitaxel, the bevacizumab flask was treated with 10  $\mu\text{g/ml}$ , and the paclitaxel/bevacizumab flask was treated with 5 nM of paclitaxel and 10  $\mu\text{g/ml}$ . The control and bevacizumab dishes showed a persistence of colonies. The paclitaxel and combination of paclitaxel and bevacizumab showed a complete absence of visible colonies.

## **b.** Proliferative assay

Upper graphic: Serial dilution of bevacizumab and paclitaxel in combination with bevacizumab were placed in 96-well microplate.

Lower graphic: the breast cancer tumor cell line GILM2 in exponential growth was exposed to increasing nanomolar concentration of paclitaxel. Paclitaxel showed a dose response curve with an estimation of  $\text{IC}_{50}$  value of 5.2.

**Figure 7a:** *In vitro* activity of paclitaxel and bevacizumab. Clonogenic Assay

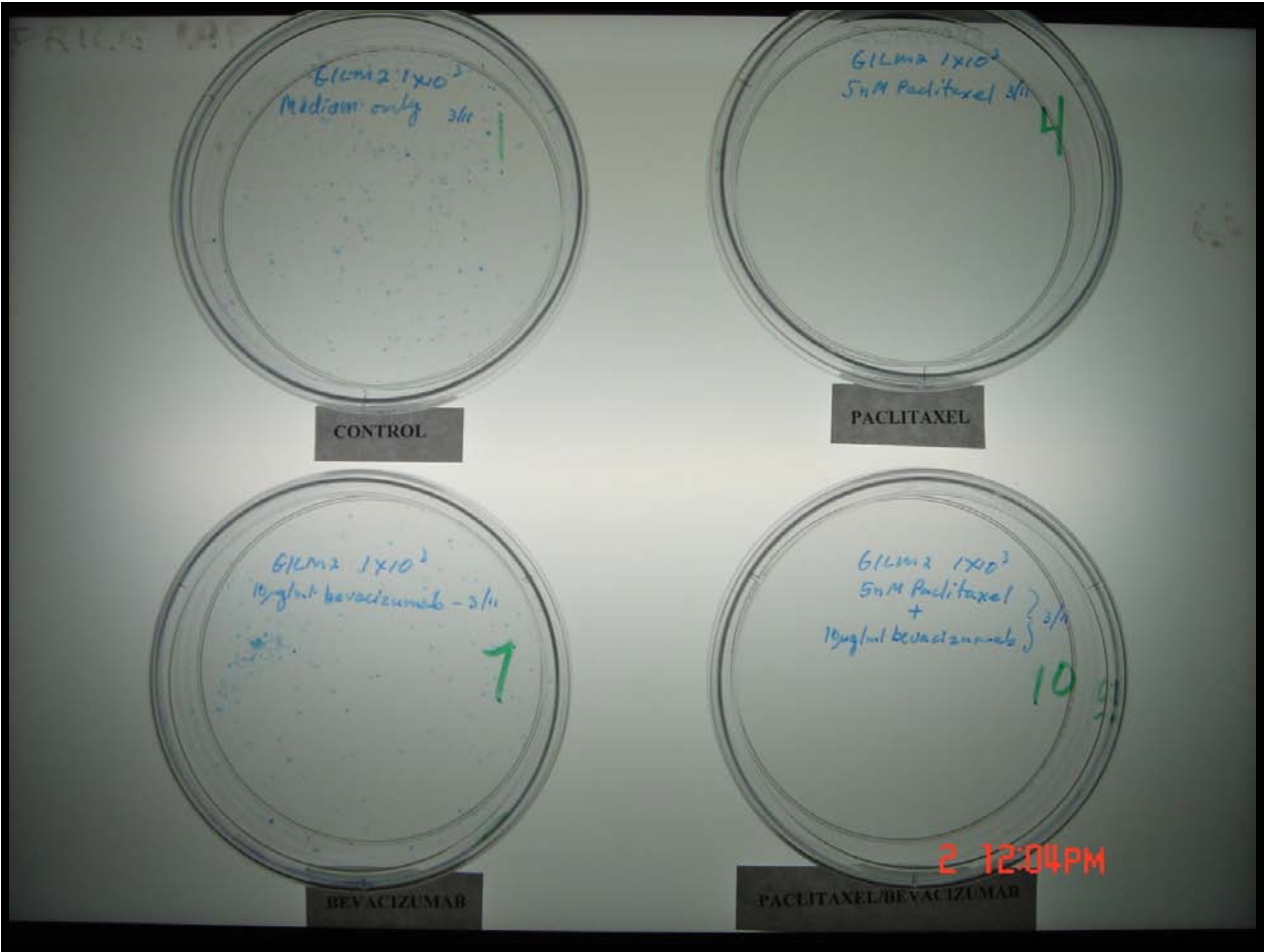
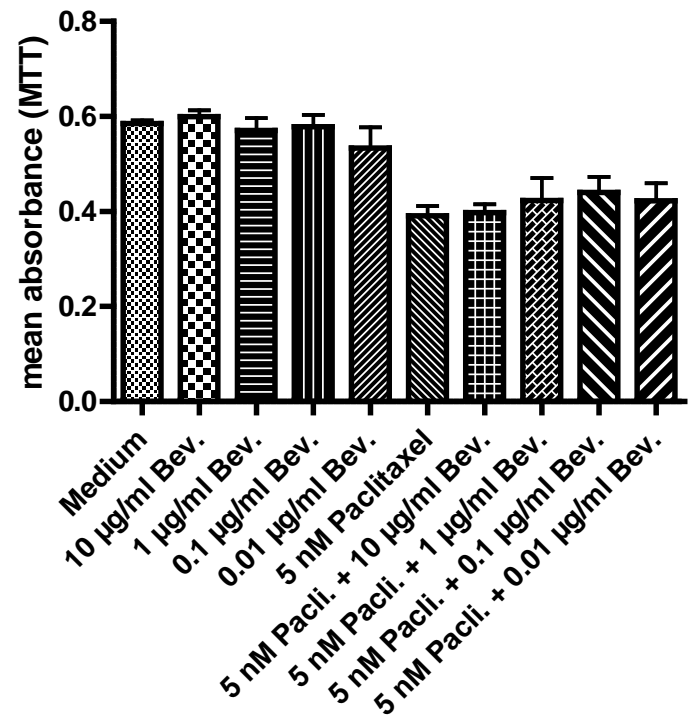
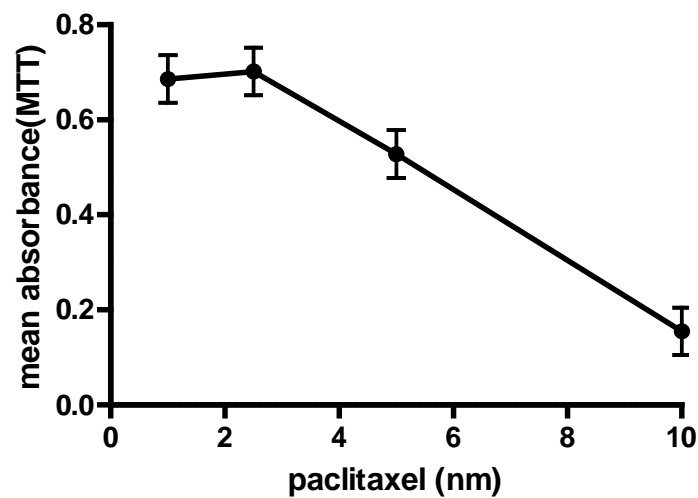


Figure 7b: GILM2 *in vitro* analysis

GILM2 sensitivity to bevacizumab and paclitaxel



GILM2 *in vitro* sensitivity to paclitaxel



## Tumor growth inhibition by the combination of paclitaxel and bevacizumab

To determine whether the treatment with paclitaxel and bevacizumab is effective to eradicate tumors *in vivo*, we conducted two independent experiments using two different chemotherapy schedules: low dose (LD) and high dose (HD). We first tested the effects of the low dose of paclitaxel (15 mg/kg) plus bevacizumab (5 mg/kg) on GILM2 tumor xenografts. Overall, the therapies were well tolerated by the mice. Compared with the control mice, a 3% to 9% weight decrease was noted in the treatment groups with the greatest decrease observed in the combination group (data not shown). No mice in any of the treatment groups appeared moribund or ill before sacrifice and no hemorrhagic or infection complications were observed. Not all mice developed primary mfp tumors (85% tumorigenicity).

*LD Experiment:* Mice treated with the combination of paclitaxel and bevacizumab inhibited tumor growth by 41% reduction mean of tumor volume of the mfp breast tumors compared with the tumors in the control group. (Figure 8 a and b) However this reduction was not statistically significant ( $t$  test  $p = 0.1720$ ). The combination of paclitaxel and bevacizumab substantially inhibited tumor growth more than either therapy alone. Paclitaxel single agent produced a reduction of 32.77% compared with control. Finally, treatment with bevacizumab produced minimal effect on the tumor control with reduction on 8% the mean of tumor volume. Tumor weight mirrored the changes observed for tumor volume (data no shown).

*HD Experiment:* Mice treated with paclitaxel and paclitaxel plus bevacizumab inhibited tumor growth by 56.1% in the mean volume of the mfp breast tumors compared with the tumors in the control group. (Figure 8 c and d) The difference of tumor volume between the

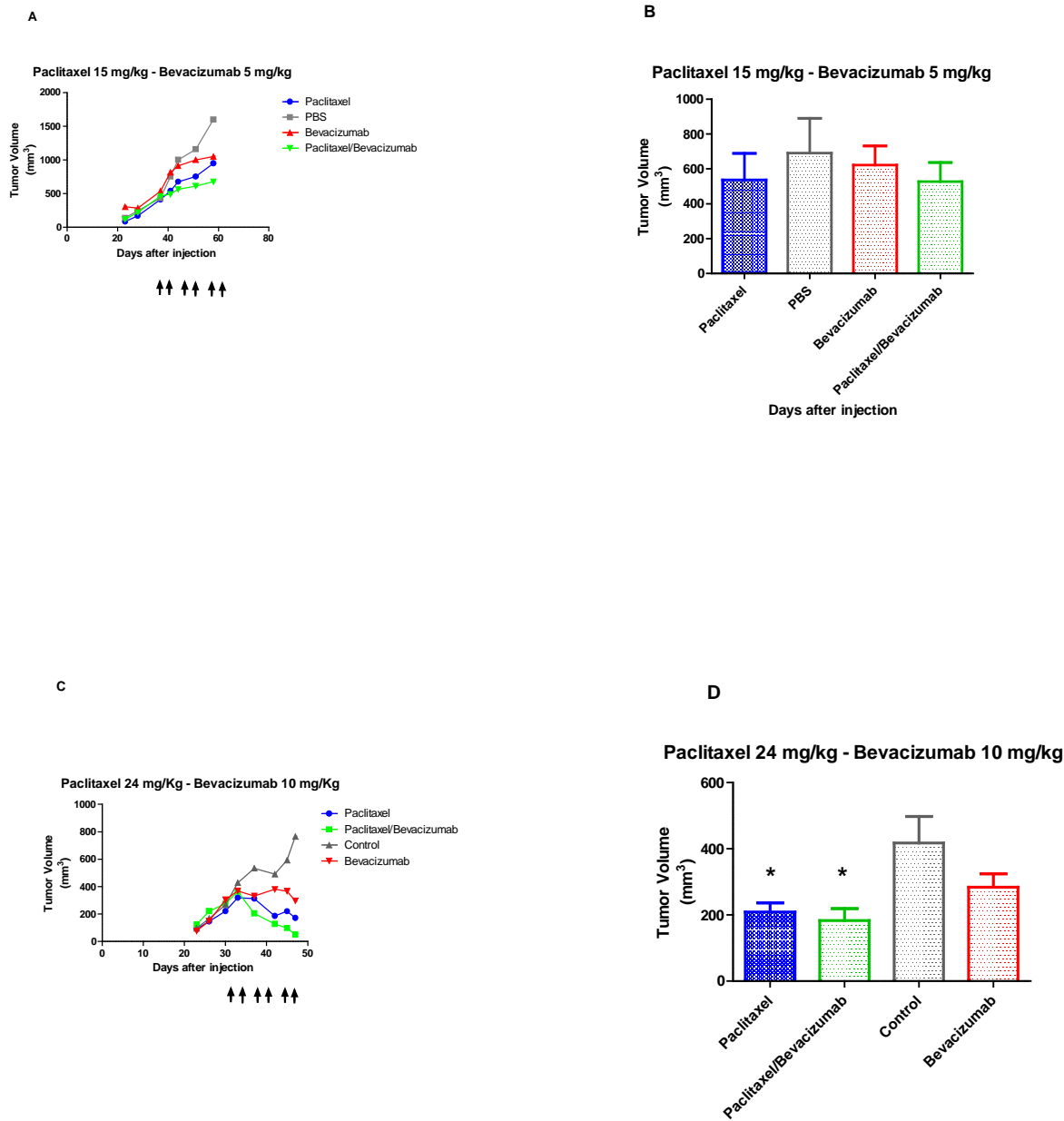


combination of paclitaxel plus bevacizumab and control group was statistically significant. ( $t$  test  $p = 0.0183$ ) The treatment with paclitaxel as single agent reduced the tumor volume by 50% ( $t$  test  $p = 0.0270$ ). Bevacizumab reduced the tumor volume by 31.9%; however, compared with control group this is not statistically significant. ( $t$  test  $p = 0.1572$ )

**Figure 8 a and b:** *In vivo* Activity of Low Dose Treatment

**Figure 8 c and d:** *In vivo* Activity of High Dose Treatment.

**Figure 8** - In vivo activity of paclitaxel and bevacizumab in GILM2 breast cancer tumor xenografts





Treatment with the combination of paclitaxel and bevacizumab decreases the tumor IFP

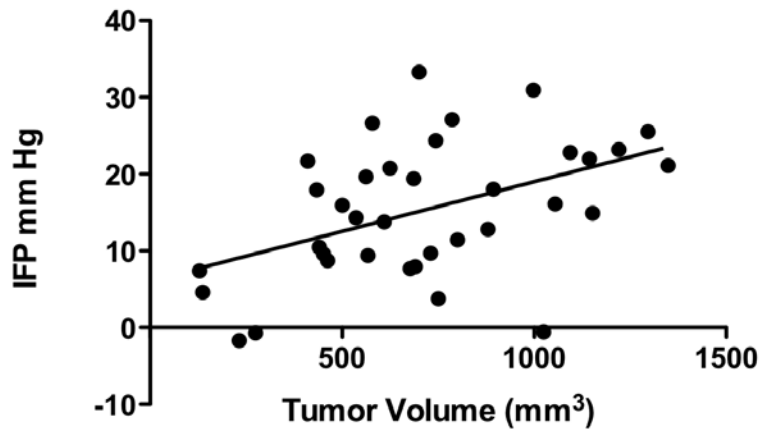
*Basal Tumor IFP*

Tumor IFP (mmHg) was evaluated in a wide range of experimental models at the baseline.

We found a positive correlation (Pearson  $r$  0.4632;  $p = 0.0044$ ) with tumor IFP and tumor volume ( $\text{mm}^3$ ) (Figure 9 a).

Figure 9

**First Experiment: correlation IFP and Tumor Volume**



Correlation Analysis	
Pearson r	0.4632
95% confidence interval	0.1587 to 0.6872
P value (two-tailed)	0.0044
R squared	0.2145

### *Effect of Treatment on Tumor IFP*

GILM2 breast cancer cells were implanted into mfp. We tested whether treatment with LD or HD decreased the tumor IFP. In the LD experiment there was no statistically significant difference between arms comparing day 1 to day 21. (Figure 9b) Tumor IFP fluctuated during treatment arms especially with paclitaxel; however, the IFP level returned to similar baseline point. In the HD group, the combination of paclitaxel and bevacizumab resulted in statistically significant reduction of IFP ( $p = 0.0068$ ) compared with the other the arms. (Figure 9 c)

**Figure 9b:** Tumor IFP in the Low Dose Group

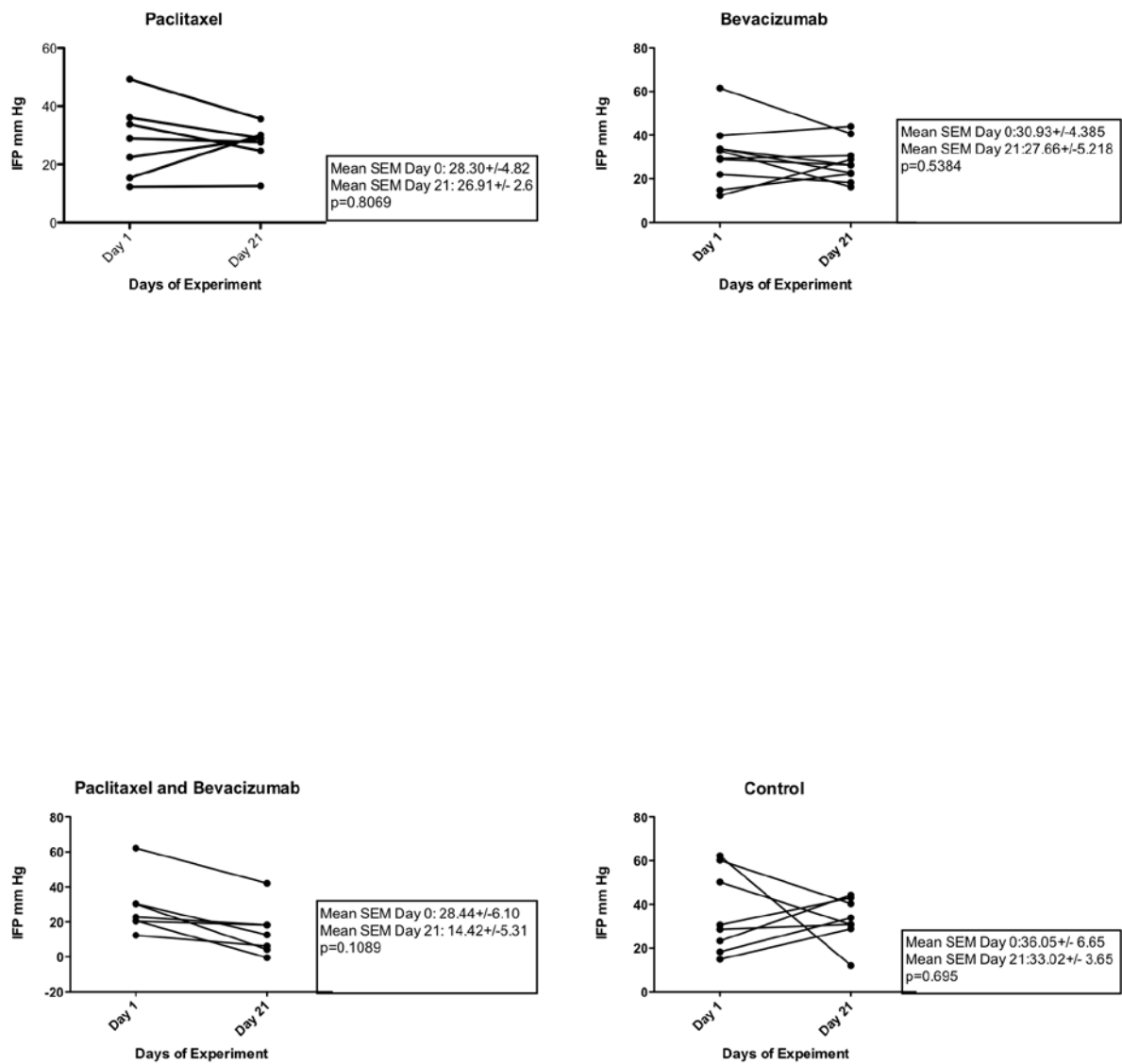
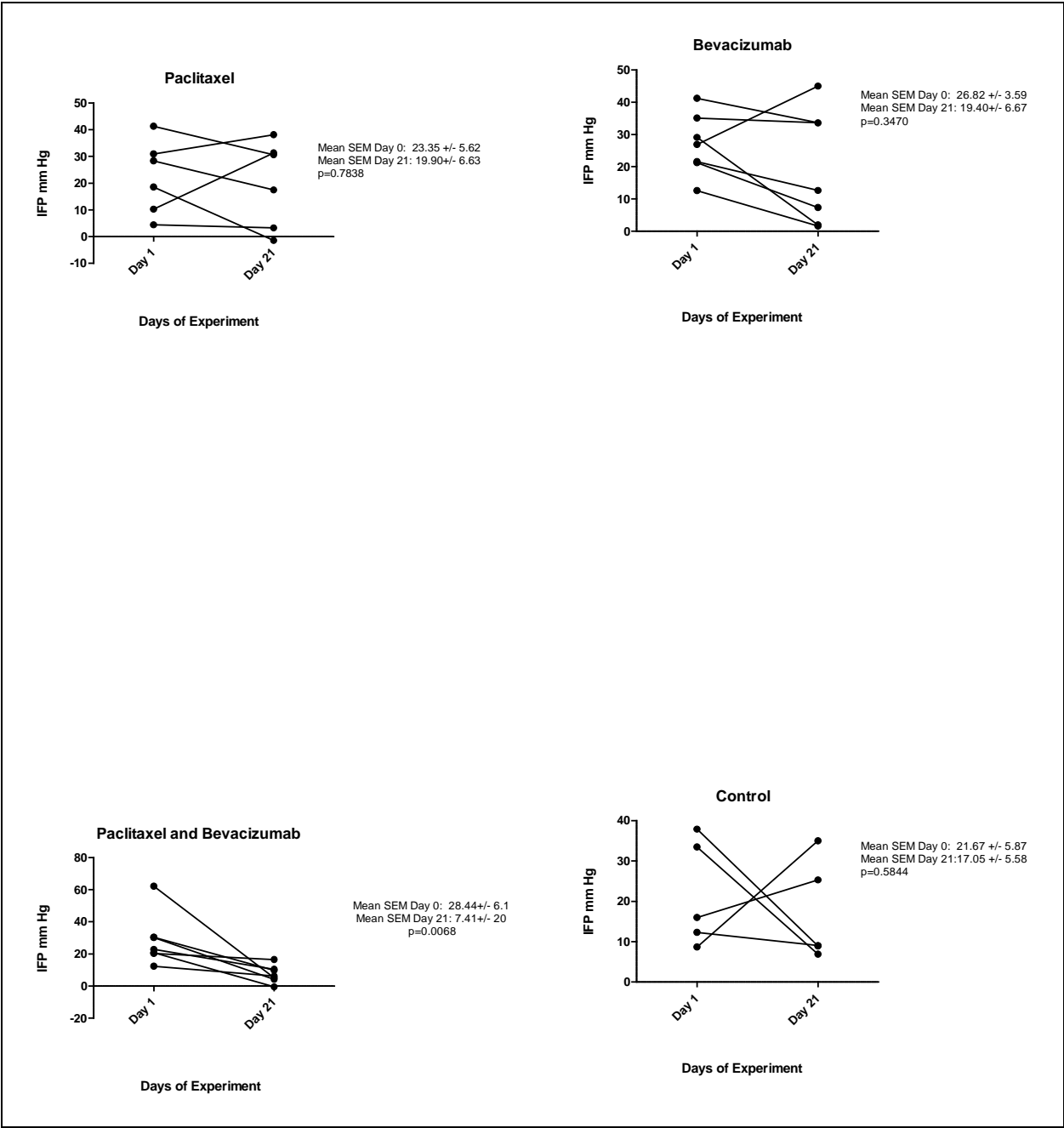




**Figure 9c: Tumor IFP in the High Dose Group**



Combination of paclitaxel and bevacizumab significantly increase tumor apoptosis.

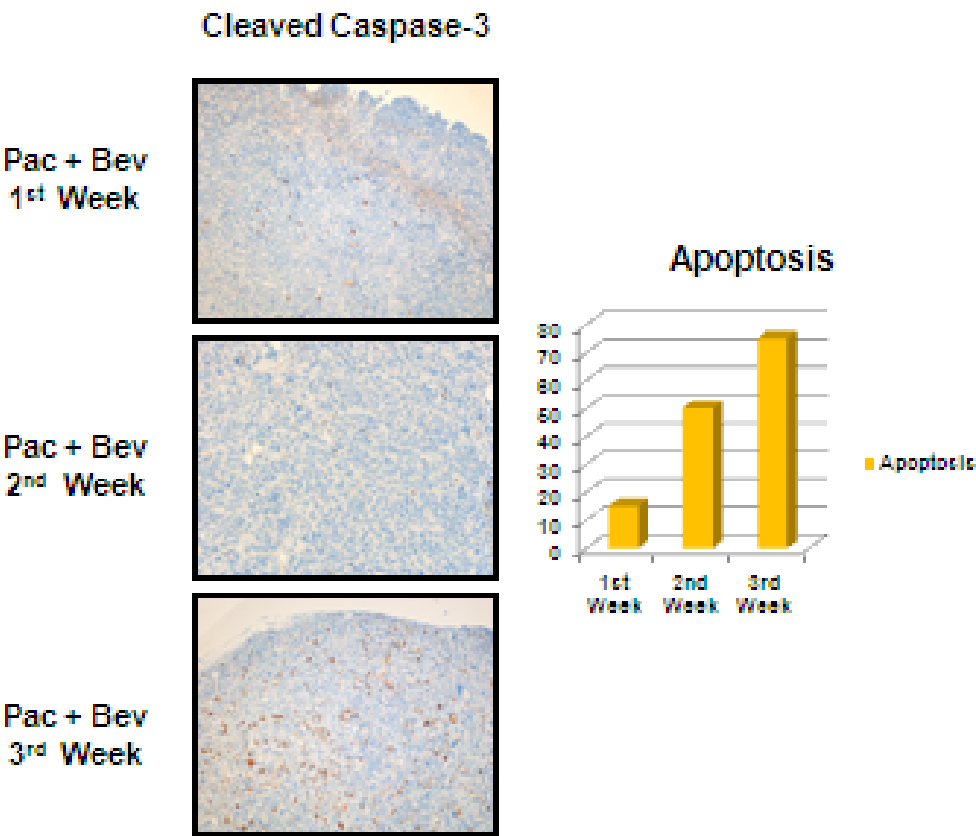
It is now clear that caspase activation (cleavage of procaspase to active caspase) is a hallmark of almost all apoptotic systems. We tested whether induction of tumor cell death might also contribute to the antitumor activity of bevacizumab in combination with paclitaxel.

These results (Fig 10) suggested that induction of apoptosis by the combination of paclitaxel and bevacizumab compared with either agent alone or vehicle, might contribute, at least in part, to the inhibition of tumor growth.

**Figure 10** - Detection of cleaved caspase 3 in apoptotic cells in paraffin sections.

Localization of cleaved caspase 3 in deparaffinized sections of formalin –fixed tissues.

Figure 10:



Combination of paclitaxel and bevacizumab increases the diameter of tumor vessels and decrease the pericyte coverage.

To assess whether neoplastic cell loss would decompress blood vessels, we measured vessel diameter in GILM2 mfp tumors. Paclitaxel increased the diameter of blood vessels at day 7, 14 and 21; however, there were no changes in vessel density. The vascular diameter of treated tumor was increased significantly when bevacizumab was added to paclitaxel, doubling the vascular diameter and indicating that the vascular surface area increased approximately by 2-fold. Next, we examined pericyte coverage using dual immunofluorescence staining for CD31 and desmin. In normal tissues we found that small vessels (venules and capillaries) were covered extensively by irregularly shaped pericytes that were associated tightly with the endothelial cells. We found that pericytes were localized in the growing tips or angiogenic “sprouts” of new blood vessels. (Figure 1 b) However, tumor vessels were morphologically abnormal and tortuous in shape with irregular pericyte coverage. Although most tumor vessels had pericyte coverage, the pericytes were attached loosely and had extensions projecting both toward the endothelial cells and the tumor stroma. After one week of treatment with paclitaxel with and without bevacizumab, there was an increase in pericytes covering the blood vessels and also extending into the tumor stroma. (Figure 11 a) The pericyte recruitment might be secondary to tissue stress after treatment with chemotherapy. Subsequently, after 2 weeks of treatment, the blood vessels become enlarged, with patchy endothelial coverage and small amounts of pericytes. (Figure 11 b) At the end of third week of treatment, the group treated with the combination of paclitaxel and bevacizumab were characterized by absence of lumen of blood vessels and practically

complete disappearance of pericytes. This effect is more pronounced in the group that received the combination of paclitaxel and bevacizumab than the group that received paclitaxel single agent. (Figure 11c) The stained area in 20 fields was quantified by using ImageJ software. Mean  $\pm$  SEM (5 mice each) are shown. \*,  $P < 0.01$  (Student's *t* test).

**Figure 11** - performed to visualize endothelial cells and pericytes. Images were taken at original magnification (X400). Pericyte coverage of small vessels in breast carcinoma. The percentages of vessels with at least 50% coverage of associated desmin-positive cells were counted.

**Figure 11a: Immunofluorescence Analysis of Paclitaxel and Paclitaxel plus Bevacizumab over Three Weeks Treatment**

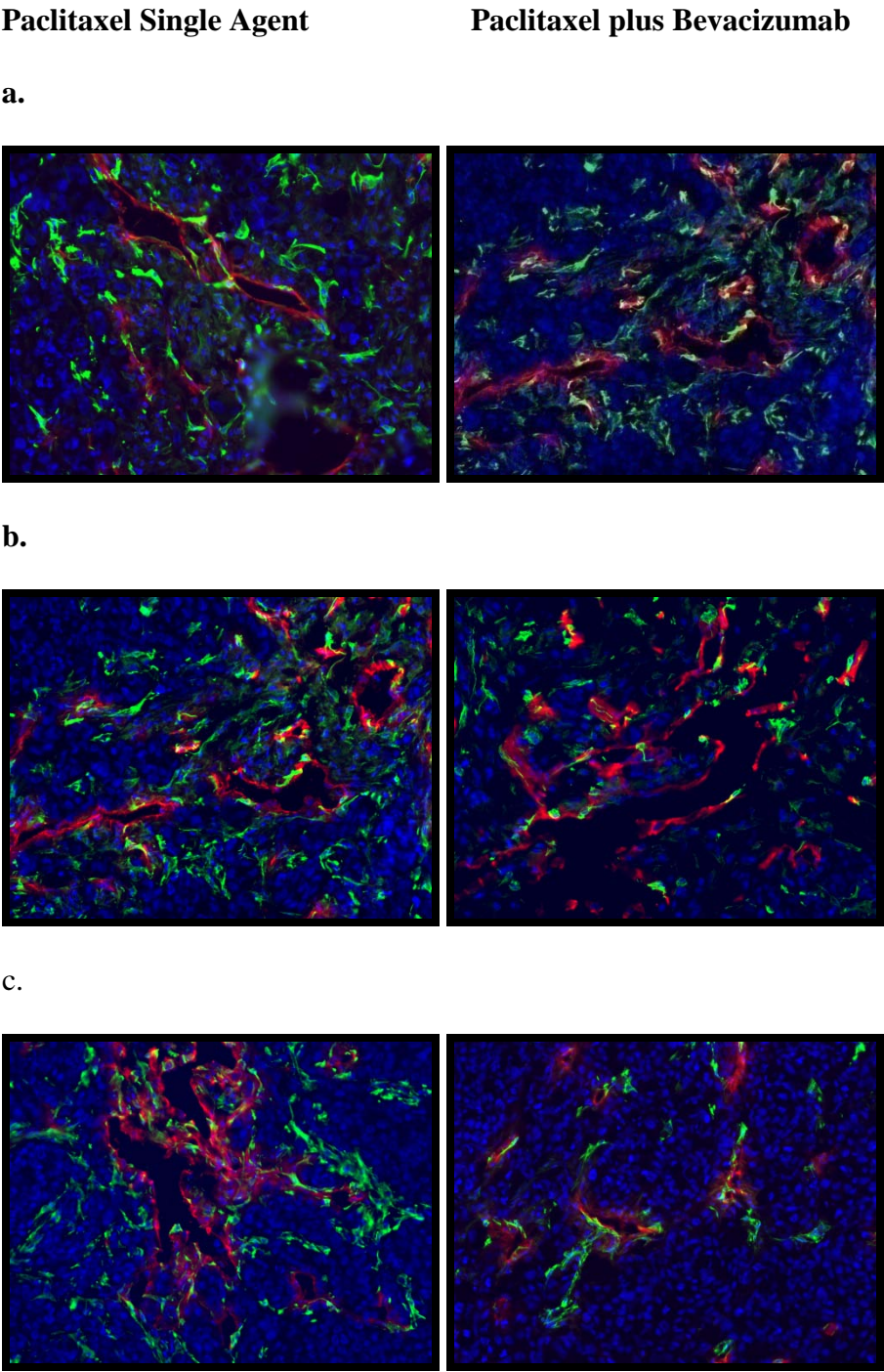




Figure 11 b: Quantification of endothelial cells, pericytes and apoptosis during the treatment with paclitaxel and bevacizumab.

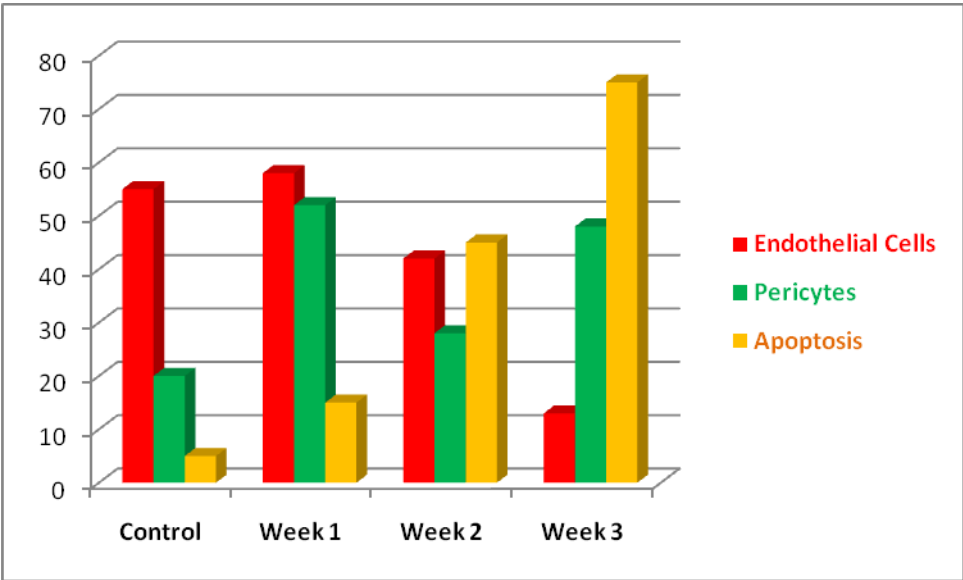
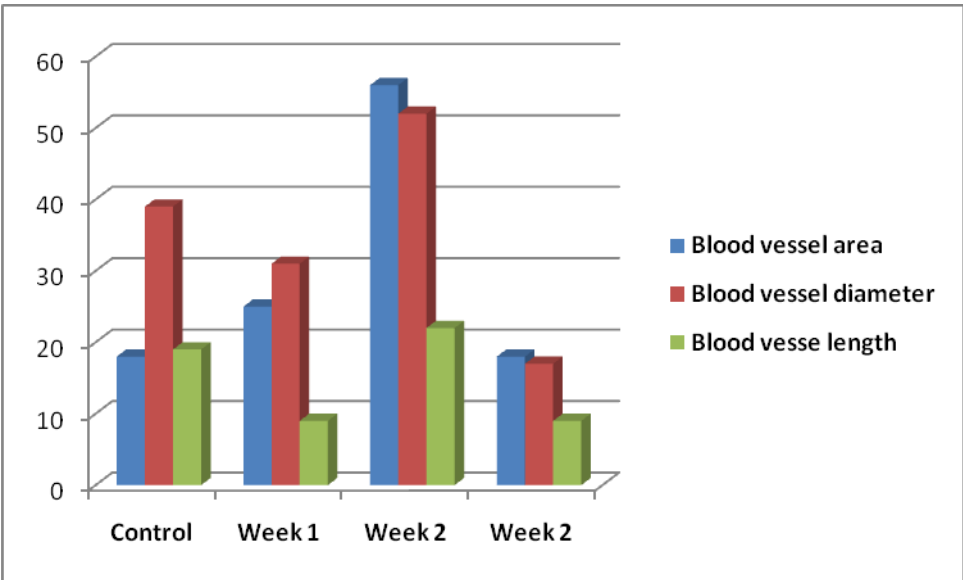


Figure 11 c: Quantification of Blood vessel characteristics.



Tumor distribution of labeled-paclitaxel improved with the addition of bevacizumab.

To assess whether pretreatment with bevacizumab is associated with tumor concentration of paclitaxel, we studied paclitaxel distribution in GILM2 tumor xenografts. The distribution of labeled-paclitaxel within GILM2 xenografts was observed by examining tumors excised at a range of time points after i.p. administration of the drug. Tumor cryosections were imaged and stained immunohistochemically for combinations of paclitaxel, and endothelial cell marker CD31 (*red*).

*Distribution of paclitaxel through tumors.* Mice bearing GILM2 xenografts were given single i.p. doses of 24 mg/kg labeled-paclitaxel. A group of mice (4 per group) received bevacizumab 10 mg/kg and other group received PBS (control). Representative high resolution composite images for whole tumor sections obtained 2 to 2.5 mm from the tumor edge were generated with a magnified portion of an untreated control tumor shown in Figure 12. Similar images of treated tumor show paclitaxel-labeled (*blue*) proximal to vasculature (CD31 in *red*)

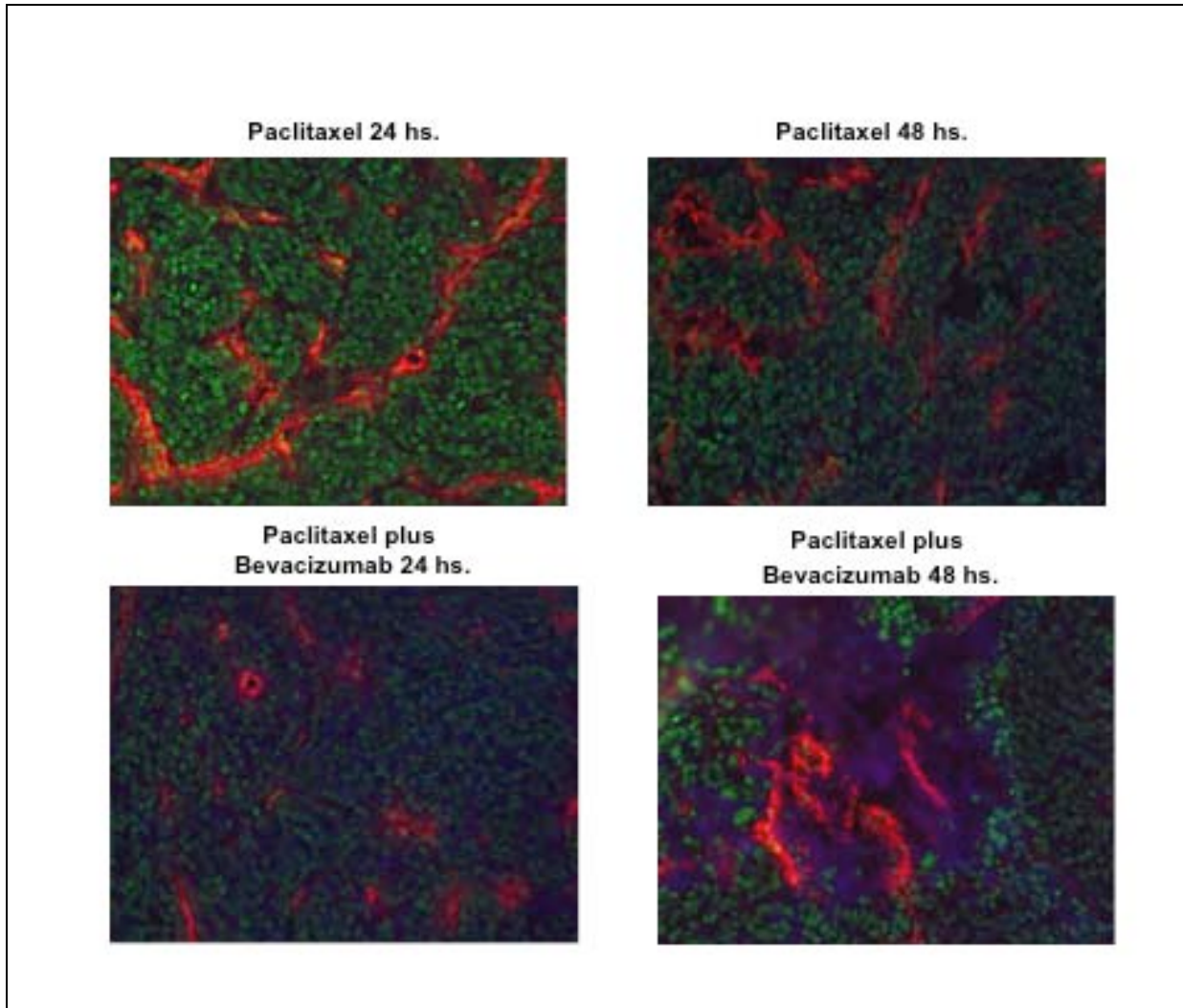
As shown in Figure 12, paclitaxel distribution into the tumor tissue was, in general, higher in the bevacizumab treated group, with the difference in mean paclitaxel tumor concentration between the groups reaching statistical significance at 24hs and 48 hs.

**Figure 12** - Distribution of labeled-paclitaxel into the tumor

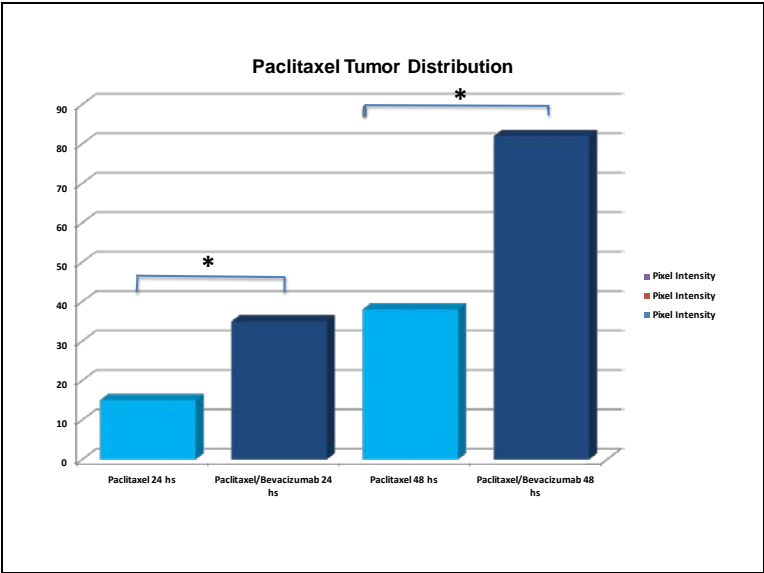
a. Labeled-paclitaxel and vessels analysis on cryosections of GILM2 xenografts tumors in paclitaxel and paclitaxel plus bevacizumab treated. Representative images show differences in vessel morphology with CD31 staining. Intratumor distribution of labeled-paclitaxel (*blue*) and nuclear staining with Cytoxgreen (*green*).

b. Graphical representation of image analysis of intratumor paclitaxel distribution. Bars represent means values  $\pm$ SEM (n = 4 per group). \*  $P < .05$ , versus control.

**a. Effect of Bevacizumab in Tissue Paclitaxel Distribution**



**b. Quantification of Labeled-Paclitaxel**



## LC/MS Analysis

In this aim, we documented the amount of paclitaxel accumulation in the tumor and this was directly analyzed by LC/MS. We used ANOVA test to determine whether or not there is a statistically significance difference among the means of two group.

### *Low Dose Experiment:*

Eighteen mice were randomized in two arms: paclitaxel 15 mg/kg, and paclitaxel (same dose) plus bevacizumab (5 mg/kg). At the end of each week, 3 mice were sacrificed and tumor removed. The comparison between the single agent paclitaxel versus the combination paclitaxel and bevacizumab was statistically significant (1 way ANOVA;  $p = 0.0457$ )

### *High Dose Experiment:*

Eighteen mice were randomized in two arms: paclitaxel 24 mg/kg, and paclitaxel (same dose) plus bevacizumab (10 mg/kg). At the end of each week, 3 mice were sacrificed and tumor removed. The comparison between the single agent paclitaxel versus the combination paclitaxel and bevacizumab was not statistically significant (1 way ANOVA;  $p = 0.2224$ )

The comparison between the LD and HD was statistically significant (1 way ANOVA;  $p = 0.0257$ )

Our conclusion of this experiment was that intratumor paclitaxel accumulation increases when low dose of paclitaxel and bevacizumab are given together compared with paclitaxel single agent. At these low doses synergistic effect was demonstrated using this drug combination. This synergistic effect was not observed when combinations of high doses of same drugs were used.

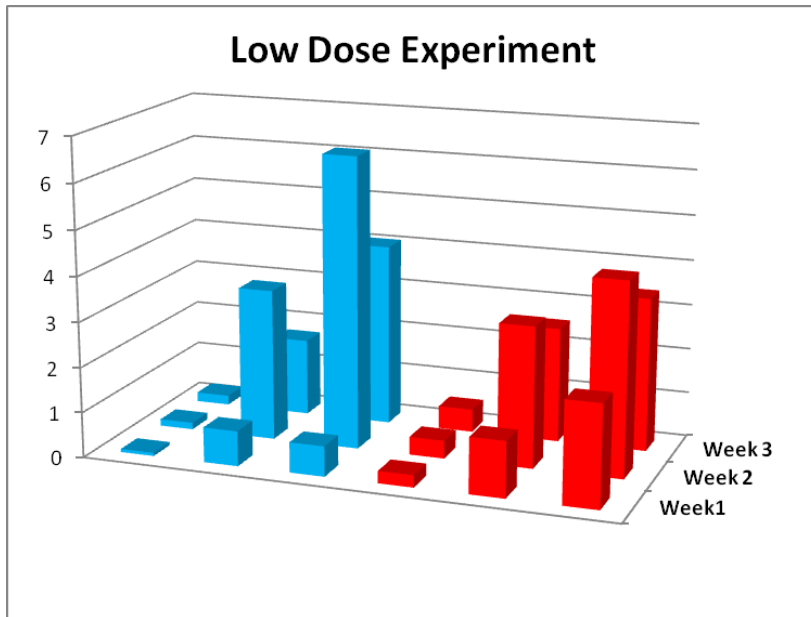
**Figure 13** - Chromatography/Mass Spectrometry (LC/MS)

Eighteen samples were collected for LD and HD treatment.

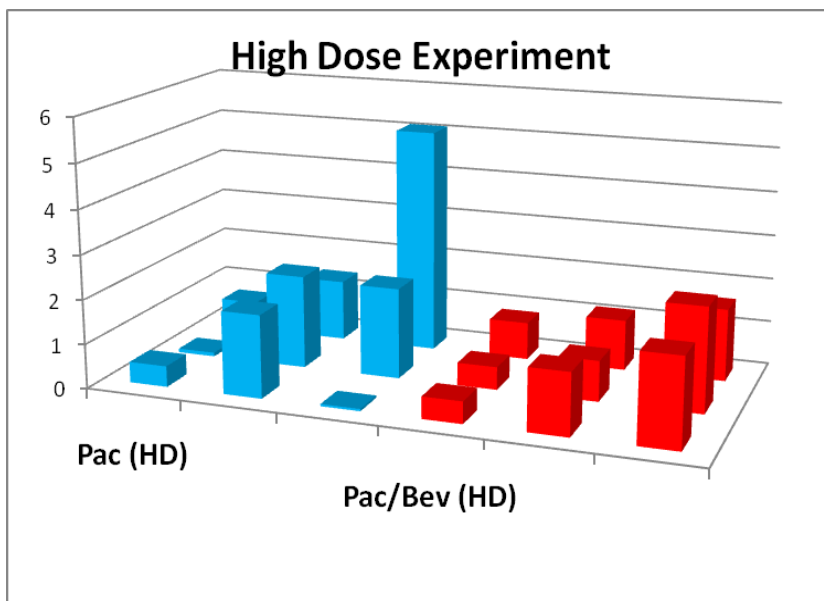
- a. Tissue paclitaxel accumulation in the low dose treatment.
- b. Tissue paclitaxel accumulation in the low dose treatment.

**Figure 13: Liquid Chromatography/Mass Spectrometry (LC/MS)**

a. Tissue paclitaxel accumulation in the low dose treatment



b. Tissue paclitaxel accumulation in the high dose treatment





## Discussion

Traditionally, cancer treatment has focused on targeting the tumor cells directly. It has, however, become clear that tumor cells interact with and are dependent on surrounding normal cell types in the tumor. So, targeting of non-malignant cell types, in parallel to the tumor cells, might represent the future of cancer treatment. Combination therapy with an antiangiogenic agent plus chemotherapy acts at multiple targets within the tumor, depriving it of nutrients and oxygen (i.e. antivascular and antiangiogenic effects) and killing highly proliferative tumor cells (i.e. cytotoxic effects) <sup>[91]</sup>.

To summarize, the studies presented in this thesis have investigated the effects of the combination of paclitaxel and bevacizumab on tumor growth, tumor IFP, transvascular transport, and tissue paclitaxel distribution. It has conclusively demonstrated that the addition of bevacizumab to paclitaxel increases the drug uptake, thus decreasing the IFP and increasing significantly the tissue apoptosis.

It is believed that in the presence of a normal vasculature paclitaxel crosses membranes by diffusion; however, in tumors, convective transport is influenced by changes in IFP. In this study, the tumor IFP decreased significantly when paclitaxel is combined with bevacizumab. In contrast to some early animal model studies demonstrating that anti-VEGF agent decreases the tumor IFP, <sup>[75]</sup> <sup>[76]</sup> our observation together with other authors <sup>[92]</sup> demonstrated that single agent of anti-VEGF (bevacizumab) does not affect the tumor IFP

Our work as well the work of others <sup>[93]</sup> has shown that tumor IFP measurements can predict tumor response in patients. The mechanisms responsible for the changes in tumor IFP

during treatment are poorly understood. This study provides insights into the interrelationship among neoplastic cells, tumor vasculature, tumor IFP, and drug uptake by the tumor.

Chemosensitization is the ability to augment the effects of standard chemotherapy. One of the possible mechanisms for chemosensitization is improving intratumoral chemotherapy concentrations by increasing total or regional delivery of chemotherapy to the tumor. This mechanism potentially leads to a decreased tumor IFP. However, results from two different groups <sup>[94, 95]</sup> demonstrated that the induction of apoptosis by the action of taxanes -docetaxel and paclitaxel, causing and decompressing blood vessels can also reduce tumor IFP. As antiangiogenic agents are generally cytostatic rather than cytoreductive, combinations involving conventional cytotoxic chemotherapies may be useful for maximizing therapeutic activity. The net outcome of a combination therapy is determined by the balance between antiangiogenic potential and cytotoxicity. In this preclinical work, we found that low dose combination of paclitaxel plus bevacizumab produces a synergistic effect with increased intra-tumor paclitaxel concentration when bevacizumab is added. In contrast, the high dose of treatment produced no statistical significant increment of paclitaxel accumulation into the tumor. But at the same time, effective tumor control was seen only with the high doses of treatment. The same effect has been seen in the clinic where improved clinical responses were observed when conventional chemotherapy is combined with low-dose of bevacizumab compared with high dose bevacizumab. <sup>[96]</sup>

There are two lines of investigation that would benefit from further studies. First, there is much to do to fully understand the mechanism behind the increased IFP of solid tumors and to find ways to lower tumor IFP. Most importantly, the concept of lowering

tumor IFP and improving tumor efficacy needs to be validated in the clinic. So far, there is only one study demonstrating that the IFP was an independent prognostic parameter to disease-free survival in cervical carcinoma patients treated with radiation therapy. A decreased IFP at early phase of the beginning of the neoadjuvant treatment can be used as early surrogate of tumor response in breast cancer patients. This effect would improve the current tumor assessment and impact in the management of breast cancer patients treated with primary systemic therapy.

Second, we need to repeat the experiment using the same preclinical protocol assessing tumor response by dynamic contrast enhanced magnetic resonance imaging (DCE-MRI). In our prior experience with DCE-MRI we found multiple technical difficulties related to the site of implantation of mfp and the experiment found no differences in blood flow and permeability, besides good tumor control in the combination arm with paclitaxel and bevacizumab. Tumor blood flow is highly heterogeneous. It is not the total blood flow, but the distribution of blood flow that determines the distribution of a drug or oxygen in tumors. Therefore, the global (total) blood flow, as estimated by the currently available resolution of DCE-MRI or CTs, does not inform us about the degree of spatial heterogeneity in vascular normalization of distribution. An alternative approach will be investigated in the future using an ultrasound Doppler to characterize the blood vessels morphology. Thus, there is real necessity to improve our imaging techniques with higher resolution of the temporal changes in blood flow and other physiological parameters. This is a real unmet need to definitively establish the effects of antiangiogenic treatment on vascular function.

Neoadjuvant chemotherapy for the treatment of breast cancer has been used for almost four decades and it is considered the initial component of the multidisciplinary approach for the treatment of patients with locally advanced and large operable breast cancer. This approach has been proven safe and as effective as adjuvant therapy. Although of the more convincing arguments for the neoadjuvant treatment its value as an in vivo test for drug sensitivity, the major advantage of this treatment modality is the increase of the breast-conservative approach. Several studies in breast cancer patients treated with neoadjuvant treatment showed that drug sensitivity correlates with survival. Several aspects of the neoadjuvant therapy remain to be confirmed and validated in prospective trials. After many years of investigations, many questions remain regarding the best chemotherapy, sequence of different regimens, and length of treatment. Recently, neoadjuvant chemotherapy provides an ideal scenario for determining prognostic and predictive factors of response to specific regimens. The pathologic complete response (pCR) is the major surrogate endpoint; however, pCR occurs several months after the initiation of neoadjuvant chemotherapy. We believe that early changes in the tumor IFP might be correlated with tumor response. A report by Milosevic and collaborators <sup>[59]</sup> has shown that the tumor IFP can predict survival in patients with cervix cancer treated by radiation therapy, independently of other clinical factors, suggesting that it is a potential useful parameter of response. Currently, I have developed an exploratory biomarker study to analyze changes in tumor IFP during neoadjuvant treatment in breast and malignant melanoma patients. I am planning to use the same IFP instrumentation for intratumor hypertension assessment that was utilized in this preclinical experiment.

The administration of single agent anti-VEGF such as bevacizumab, sorafenib and sunitinib has demonstrated a modest tumor activity in MBC with responses rate of 6%, 2%, and 11%, respectively. Results from phase III clinical trials demonstrated that bevacizumab in combination with chemotherapy had clinical benefit in previously untreated breast, lung and colorectal cancer when compared with standard chemotherapy alone.<sup>[97-99]</sup> Although three large randomized clinical trials in advanced breast cancer patients using paclitaxel plus bevacizumab have demonstrated positive results increasing consistently the progression free survival, the FDA has recently questioned the efficacy of bevacizumab. Several preclinical studies using animal models have demonstrated that the combination of anti-angiogenic agent with cytotoxic drug is superior compared with single agent treatment. After two years working with animal models using different combination of the aforementioned drugs, this study suggests that bevacizumab might modify temporarily the transvascular transport of the cytotoxic agent, thus acting as chemosensitizer more than cytostasis.

## BIBLIOGRAPHY

- 1 Jemal A, Siegel R, Ward E, Murray T, Xu J, Thun MJ: Cancer statistics, 2007. *CA Cancer J Clin* 2007;57:43-66.
- 2 Jemal A, Siegel R, Xu J, Ward E: Cancer statistics, 2010. *CA Cancer J Clin*;60:277-300.
- 3 Garcia M, Jemal A, Ward E: Global cancer facts and figures 2007.
- 4 Ravdin P, Cronin KA, Howlader N, Berg CD, Chlebowski R, Feuer EJ, Edwards BK, Berry DA: The decrease in breast-cancer incidence in 2003 in the united states. *N Engl J Med* 2007;356:1670-1674.
- 5 Giordano SH, Buzdar AU, Smith TL, Kau SW, Yang Y, Hortobagyi GN: Is breast cancer survival improving? *Cancer* 2004;100:44-52.
- 6 Fumoleau P, Delgado FM, Delozier T, Monnier A, Gil Delgado MA, Kerbrat P, Garcia-Giralt E, Keiling R, Namer M, Closon MT, et al.: Phase ii trial of weekly intravenous vinorelbine in first-line advanced breast cancer chemotherapy. *J Clin Oncol* 1993;11:1245-1252.
- 7 Livingston RB, Ellis GK, Gralow JR, Williams MA, White R, McGuirt C, Adamkiewicz BB, Long CA: Dose-intensive vinorelbine with concurrent granulocyte colony-stimulating factor support in paclitaxel-refractory metastatic breast cancer. *J Clin Oncol* 1997;15:1395-1400.
- 8 Albain KS, Nag SM, Calderillo-Ruiz G, Jordaan JP, Llombart AC, Pluzanska A, Rolski J, Melemed AS, Reyes-Vidal JM, Sekhon JS, Simms L, O'Shaughnessy J: Gemcitabine plus paclitaxel versus paclitaxel monotherapy in patients with metastatic breast cancer and prior anthracycline treatment. *J Clin Oncol* 2008;26:3950-3957.

- 9 Blum JL, Jones SE, Buzdar AU, LoRusso PM, Kuter I, Vogel C, Osterwalder B, Burger HU, Brown CS, Griffin T: Multicenter phase ii study of capecitabine in paclitaxel-refractory metastatic breast cancer. *J Clin Oncol* 1999;17:485-493.
- 10 O'Shaughnessy JA: Potential of capecitabine as first-line therapy for metastatic breast cancer: Dosing recommendations in patients with diminished renal function. *Ann Oncol* 2002;13:983.
- 11 Gradishar WJ, Tjulandin S, Davidson N, Shaw H, Desai N, Bhar P, Hawkins M, O'Shaughnessy J: Phase iii trial of nanoparticle albumin-bound paclitaxel compared with polyethylated castor oil-based paclitaxel in women with breast cancer. *J Clin Oncol* 2005;23:7794-7803.
- 12 Low JA, Wedam SB, Lee JJ, Berman AW, Brufsky A, Yang SX, Poruchynsky MS, Steinberg SM, Mannan N, Fojo T, Swain SM: Phase ii clinical trial of ixabepilone (bms-247550), an epothilone b analog, in metastatic and locally advanced breast cancer. *J Clin Oncol* 2005;23:2726-2734.
- 13 Thomas E, Tabernero J, Fornier M, Conte P, Fumoleau P, Lluch A, Vahdat LT, Bunnell CA, Burris HA, Viens P, Baselga J, Rivera E, Guarneri V, Poulart V, Klimovsky J, Lebwohl D, Martin M: Phase ii clinical trial of ixabepilone (bms-247550), an epothilone b analog, in patients with taxane-resistant metastatic breast cancer. *J Clin Oncol* 2007;25:3399-3406.
- 14 Perez EA, Lerzo G, Pivot X, Thomas E, Vahdat L, Bosserman L, Viens P, Cai C, Mullaney B, Peck R, Hortobagyi GN: Efficacy and safety of ixabepilone (bms-247550) in a phase ii study of patients with advanced breast cancer resistant to an anthracycline, a taxane, and capecitabine. *J Clin Oncol* 2007;25:3407-3414.

- 15 Roche H, Yelle L, Cognetti F, Mauriac L, Bunnell C, Sparano J, Kerbrat P, Delord JP, Vahdat L, Peck R, Lebwohl D, Ezzeddine R, Cure H: Phase ii clinical trial of ixabepilone (bms-247550), an epothilone b analog, as first-line therapy in patients with metastatic breast cancer previously treated with anthracycline chemotherapy. *J Clin Oncol* 2007;25:3415-3420.
- 16 Arriagada R, Spielmann M, Koscielny S, Le Chevalier T, Delozier T, Ducourtieux M, Tursz T, Hill C: Patterns of failure in a randomized trial of adjuvant chemotherapy in postmenopausal patients with early breast cancer treated with tamoxifen. *Ann Oncol* 2002;13:1378-1386.
- 17 American Cancer Society: Cancer facts and figures. Atlanta, American Cancer Society, 2008.
- 18 Gottesman MM: Mechanisms of cancer drug resistance. *Annu Rev Med* 2002;53:615-627.
- 19 Tannock IF: Tumor physiology and drug resistance. *Cancer Metastasis Rev* 2001;20:123-132.
- 20 Longley DB, Johnston PG: Molecular mechanisms of drug resistance. *J Pathol* 2005;205:275-292.
- 21 Paget S: The distribution of secondary growths in cancer of the breast. *Lancet* 1889;571-573.
- 22 Talmadge JE, Fidler IJ: Aacr centennial series: The biology of cancer metastasis: Historical perspective. *Cancer Res*;70:5649-5669.
- 23 Dvorak HF: Tumors: Wounds that do not heal. Similarities between tumor stroma generation and wound healing. *N Engl J Med* 1986;315:1650-1659.



- 24 Liotta LA, Kohn EC: The microenvironment of the tumour-host interface. *Nature* 2001;411:375-379.
- 25 Carmeliet P, Collen D: Molecular basis of angiogenesis. Role of vegf and ve-cadherin. *Ann N Y Acad Sci* 2000;902:249-262; discussion 262-244.
- 26 Hanahan D, Weinberg RA: The hallmarks of cancer. *Cell* 2000;100:57-70.
- 27 Cairns R, Papandreou I, Denko N: Overcoming physiologic barriers to cancer treatment by molecularly targeting the tumor microenvironment. *Mol Cancer Res* 2006;4:61-70.
- 28 Beacham DA, Lian J, Wu G, Konkle BA, Ludlow LB, Shapiro SS: Arterial shear stress stimulates surface expression of the endothelial glycoprotein ib complex. *J Cell Biochem* 1999;73:508-521.
- 29 Tredan O, Galmarini CM, Patel K, Tannock IF: Drug resistance and the solid tumor microenvironment. *J Natl Cancer Inst* 2007;99:1441-1454.
- 30 Minchinton AI, Tannock IF: Drug penetration in solid tumours. *Nat Rev Cancer* 2006;6:583-592.
- 31 Vaupel P: Tumor microenvironmental physiology and its implications for radiation oncology. *Semin Radiat Oncol* 2004;14:198-206.
- 32 Brown JM, Giaccia AJ: The unique physiology of solid tumors: Opportunities (and problems) for cancer therapy. *Cancer Res* 1998;58:1408-1416.
- 33 Brizel DM, Scully SP, Harrelson JM, Layfield LJ, Bean JM, Prosnitz LR, Dewhirst MW: Tumor oxygenation predicts for the likelihood of distant metastases in human soft tissue sarcoma. *Cancer Res* 1996;56:941-943.

- 34 Fyles A, Milosevic M, Hedley D, Pintilie M, Levin W, Manchul L, Hill RP: Tumor hypoxia has independent predictor impact only in patients with node-negative cervix cancer. *J Clin Oncol* 2002;20:680-687.
- 35 Nordsmark M, Overgaard J: Tumor hypoxia is independent of hemoglobin and prognostic for loco-regional tumor control after primary radiotherapy in advanced head and neck cancer. *Acta Oncol* 2004;43:396-403.
- 36 Wang GL, Jiang BH, Rue EA, Semenza GL: Hypoxia-inducible factor 1 is a basic-helix-loop-helix-pas heterodimer regulated by cellular o<sub>2</sub> tension. *Proc Natl Acad Sci U S A* 1995;92:5510-5514.
- 37 Semenza GL: Hypoxia-inducible factor 1: Master regulator of o<sub>2</sub> homeostasis. *Curr Opin Genet Dev* 1998;8:588-594.
- 38 Cairns RA, Papandreou I, Sutphin PD, Denko NC: Metabolic targeting of hypoxia and hif1 in solid tumors can enhance cytotoxic chemotherapy. *Proc Natl Acad Sci U S A* 2007;104:9445-9450.
- 39 Bos R, van der Groep P, Greijer AE, Shvarts A, Meijer S, Pinedo HM, Semenza GL, van Diest PJ, van der Wall E: Levels of hypoxia-inducible factor-1alpha independently predict prognosis in patients with lymph node negative breast carcinoma. *Cancer* 2003;97:1573-1581.
- 40 Yamagata M, Hasuda K, Stamato T, Tannock IF: The contribution of lactic acid to acidification of tumours: Studies of variant cells lacking lactate dehydrogenase. *Br J Cancer* 1998;77:1726-1731.

- 41 Helmlinger G, Sckell A, Dellian M, Forbes NS, Jain RK: Acid production in glycolysis-impaired tumors provides new insights into tumor metabolism. *Clin Cancer Res* 2002;8:1284-1291.
- 42 Gerweck LE, Seetharaman K: Cellular pH gradient in tumor versus normal tissue: Potential exploitation for the treatment of cancer. *Cancer Res* 1996;56:1194-1198.
- 43 Aukland K, Reed RK: Interstitial-lymphatic mechanisms in the control of extracellular fluid volume. *Physiol Rev* 1993;73:1-78.
- 44 Reed RK, Berg A, Gjerde EA, Rubin K: Control of interstitial fluid pressure: Role of beta1-integrins. *Semin Nephrol* 2001;21:222-230.
- 45 Wiig H, Rubin K, Reed RK: New and active role of the interstitium in control of interstitial fluid pressure: Potential therapeutic consequences. *Acta Anaesthesiol Scand* 2003;47:111-121.
- 46 Starling EH: On the absorption of fluids from the connective tissue spaces. *J Physiol* 1896;19:312-326.
- 47 Lund T, Onarheim H, Reed RK: Pathogenesis of edema formation in burn injuries. *World J Surg* 1992;16:2-9.
- 48 McMaster PD: The pressure and interstitial resistance prevailing in the normal and edematous skin of animals and man. *J Exp Med* 1946;84:473-494.
- 49 Hargens AR, Mubarak SJ, Owen CA, Garetto LP, Akeson WH: Interstitial fluid pressure in muscle and compartment syndromes in man. *Microvasc Res* 1977;14:1-10.
- 50 Young JS, Lumsden CE, Stalker AL: The significance of the tissue pressure of normal testicular and of neoplastic (brown-pearce carcinoma) tissue in the rabbit. *J Pathol Bacteriol* 1950;62:313-333.

- 51 Boucher Y, Kirkwood JM, Opacic D, Desantis M, Jain RK: Interstitial hypertension in superficial metastatic melanomas in humans. *Cancer Res* 1991;51:6691-6694.
- 52 Gutmann R, Leunig M, Feyh J, Goetz AE, Messmer K, Kastenbauer E, Jain RK: Interstitial hypertension in head and neck tumors in patients: Correlation with tumor size. *Cancer Res* 1992;52:1993-1995.
- 53 Lee CG, Heijn M, di Tomaso E, Griffon-Etienne G, Ancukiewicz M, Koike C, Park KR, Ferrara N, Jain RK, Suit HD, Boucher Y: Anti-vascular endothelial growth factor treatment augments tumor radiation response under normoxic or hypoxic conditions. *Cancer Res* 2000;60:5565-5570.
- 54 Brekken C, Bruland OS, de Lange Davies C: Interstitial fluid pressure in human osteosarcoma xenografts: Significance of implantation site and the response to intratumoral injection of hyaluronidase. *Anticancer Res* 2000;20:3503-3512.
- 55 Stohrer M, Boucher Y, Stangassinger M, Jain RK: Oncotic pressure in solid tumors is elevated. *Cancer Res* 2000;60:4251-4255.
- 56 Rubin K, Sjoquist M, Gustafsson AM, Isaksson B, Salvessen G, Reed RK: Lowering of tumoral interstitial fluid pressure by prostaglandin e(1) is paralleled by an increased uptake of (51)cr-edta. *Int J Cancer* 2000;86:636-643.
- 57 Curnis F, Sacchi A, Corti A: Improving chemotherapeutic drug penetration in tumors by vascular targeting and barrier alteration. *J Clin Invest* 2002;110:475-482.
- 58 Roh HD, Boucher Y, Kalnicki S, Buchsbaum R, Bloomer WD, Jain RK: Interstitial hypertension in carcinoma of uterine cervix in patients: Possible correlation with tumor oxygenation and radiation response. *Cancer Res* 1991;51:6695-6698.

- 59 Milosevic M, Fyles A, Hedley D, Pintilie M, Levin W, Manchul L, Hill R: Interstitial fluid pressure predicts survival in patients with cervix cancer independent of clinical prognostic factors and tumor oxygen measurements. *Cancer Res* 2001;61:6400-6405.
- 60 Alvarez RH, Kantarjian HM, Cortes JE: Biology of platelet-derived growth factor and its involvement in disease. *Mayo Clin Proc* 2006;81:1241-1257.
- 61 Ostman A, Heldin CH: Involvement of platelet-derived growth factor in disease: Development of specific antagonists. *Adv Cancer Res* 2001;80:1-38.
- 62 Okuda K, Weisberg E, Gilliland DG, Griffin JD: Arg tyrosine kinase activity is inhibited by sti571. *Blood* 2001;97:2440-2448.
- 63 Pietras K, Ostman A, Sjoquist M, Buchdunger E, Reed RK, Heldin CH, Rubin K: Inhibition of platelet-derived growth factor receptors reduces interstitial hypertension and increases transcapillary transport in tumors. *Cancer Res* 2001;61:2929-2934.
- 64 Pietras K, Rubin K, Sjoblom T, Buchdunger E, Sjoquist M, Heldin CH, Ostman A: Inhibition of pdgf receptor signaling in tumor stroma enhances antitumor effect of chemotherapy. *Cancer Res* 2002;62:5476-5484.
- 65 Pietras K, Stumm M, Hubert M, Buchdunger E, Rubin K, Heldin CH, McSheehy P, Wartmann M, Ostman A: Sti571 enhances the therapeutic index of epothilone b by a tumor-selective increase of drug uptake. *Clin Cancer Res* 2003;9:3779-3787.
- 66 Pietras K, Sjoblom T, Rubin K, Heldin CH, Ostman A: Pdgf receptors as cancer drug targets. *Cancer Cell* 2003;3:439-443.
- 67 Jain RK: Transport of molecules across tumor vasculature. *Cancer Metastasis Rev* 1987;6:559-593.

- 68 Heldin CH, Rubin K, Pietras K, Ostman A: High interstitial fluid pressure - an obstacle in cancer therapy. *Nat Rev Cancer* 2004;4:806-813.
- 69 Boucher Y, Jain RK: Microvascular pressure is the principal driving force for interstitial hypertension in solid tumors: Implications for vascular collapse. *Cancer Res* 1992;52:5110-5114.
- 70 Curti BD, Urba WJ, Alvord WG, Janik JE, Smith JW, 2nd, Madara K, Longo DL: Interstitial pressure of subcutaneous nodules in melanoma and lymphoma patients: Changes during treatment. *Cancer Res* 1993;53:2204-2207.
- 71 Less JR, Posner MC, Boucher Y, Borochovit D, Wolmark N, Jain RK: Interstitial hypertension in human breast and colorectal tumors. *Cancer Res* 1992;52:6371-6374.
- 72 Baxter LT, Jain RK: Transport of fluid and macromolecules in tumors. I. Role of interstitial pressure and convection. *Microvasc Res* 1989;37:77-104.
- 73 Jain RK: Transport of molecules in the tumor interstitium: A review. *Cancer Res* 1987;47:3039-3051.
- 74 Boucher Y, Salehi H, Witwer B, Harsh GRt, Jain RK: Interstitial fluid pressure in intracranial tumours in patients and in rodents. *Br J Cancer* 1997;75:829-836.
- 75 Griffon-Etienne G, Boucher Y, Brekken C, Suit HD, Jain RK: Taxane-induced apoptosis decompresses blood vessels and lowers interstitial fluid pressure in solid tumors: Clinical implications. *Cancer Res* 1999;59:3776-3782.
- 76 Milas L, Hunter NR, Mason KA, Milross CG, Saito Y, Peters LJ: Role of reoxygenation in induction of enhancement of tumor radioresponse by paclitaxel. *Cancer Res* 1995;55:3564-3568.

- 77 Senger DR, Galli SJ, Dvorak AM, Perruzzi CA, Harvey VS, Dvorak HF: Tumor cells secrete a vascular permeability factor that promotes accumulation of ascites fluid. *Science* 1983;219:983-985.
- 78 Tong RT, Boucher Y, Kozin SV, Winkler F, Hicklin DJ, Jain RK: Vascular normalization by vascular endothelial growth factor receptor 2 blockade induces a pressure gradient across the vasculature and improves drug penetration in tumors. *Cancer Res* 2004;64:3731-3736.
- 79 Willett CG, Boucher Y, di Tomaso E, Duda DG, Munn LL, Tong RT, Chung DC, Sahani DV, Kalva SP, Kozin SV, Mino M, Cohen KS, Scadden DT, Hartford AC, Fischman AJ, Clark JW, Ryan DP, Zhu AX, Blaszkowsky LS, Chen HX, Shellito PC, Lauwers GY, Jain RK: Direct evidence that the vegf-specific antibody bevacizumab has antivascular effects in human rectal cancer. *Nat Med* 2004;10:145-147.
- 80 Gee MS, Procopio WN, Makonnen S, Feldman MD, Yeilding NM, Lee WM: Tumor vessel development and maturation impose limits on the effectiveness of anti-vascular therapy. *Am J Pathol* 2003;162:183-193.
- 81 Bergers G, Song S, Meyer-Morse N, Bergsland E, Hanahan D: Benefits of targeting both pericytes and endothelial cells in the tumor vasculature with kinase inhibitors. *J Clin Invest* 2003;111:1287-1295.
- 82 Hurst J, Maniar N, Tombarkiewicz J, Lucas F, Roberson C, Steplewski Z, James W, Perras J: A novel model of a metastatic human breast tumour xenograft line. *Br J Cancer* 1993;68:274-276.

- 83 Lev DC, Kiriakova G, Price JE: Selection of more aggressive variants of the gi101a human breast cancer cell line: A model for analyzing the metastatic phenotype of breast cancer. *Clin Exp Metastasis* 2003;20:515-523.
- 84 Kluger HM, Chelouche Lev D, Kluger Y, McCarthy MM, Kiriakova G, Camp RL, Rimm DL, Price JE: Using a xenograft model of human breast cancer metastasis to find genes associated with clinically aggressive disease. *Cancer Res* 2005;65:5578-5587.
- 85 Ozerdem U, Hargens AR: A simple method for measuring interstitial fluid pressure in cancer tissues. *Microvasc Res* 2005;70:116-120.
- 86 Chelouche-Lev D, Miller CP, Tellez C, Ruiz M, Bar-Eli M, Price JE: Different signalling pathways regulate vegf and il-8 expression in breast cancer: Implications for therapy. *Eur J Cancer* 2004;40:2509-2518.
- 87 Olive PL, Banath JP, Aquino-Parsons C: Measuring hypoxia in solid tumours--is there a gold standard? *Acta Oncol* 2001;40:917-923.
- 88 Tong X, Zhou J, Tan Y: Liquid chromatography/tandem triple-quadrupole mass spectrometry for determination of paclitaxel in rat tissues. *Rapid Commun Mass Spectrom* 2006;20:1905-1912.
- 89 Wang X, Pang J, Newman RA, Kerwin SM, Bowman PD, Stavchansky S: Quantitative determination of fluorinated caffeic acid phenethyl ester derivative from rat blood plasma by liquid chromatography-electrospray ionization tandem mass spectrometry. *J Chromatogr B Analyt Technol Biomed Life Sci* 2008;867:138-143.
- 90 Kempen EC, Yang P, Felix E, Madden T, Newman RA: Simultaneous quantification of arachidonic acid metabolites in cultured tumor cells using high-performance liquid



- chromatography/electrospray ionization tandem mass spectrometry. *Anal Biochem* 2001;297:183-190.
- 91 Teicher BA: A systems approach to cancer therapy. (antioncogenics + standard cytotoxics-->mechanism(s) of interaction). *Cancer Metastasis Rev* 1996;15:247-272.
  - 92 Kasman I, Bagri A, Mak J, Peale F, Carano R, Ross J, Berry L, Shin Y, Rudewicz P, Austin C, Ferrando R, Ross S, Crocker L, Van Bruggen N, Pais H, Scudder K, Hollister B, Plowman G: Mechanistic evaluation of the combination effect of anti-vegf and chemotherapy: AACR Meeting, 2008,
  - 93 Ferretti S, Allegrini PR, Becquet MM, McSheehy PM: Tumor interstitial fluid pressure as an early-response marker for anticancer therapeutics. *Neoplasia* 2009;11:874-881.
  - 94 Padera TP, Stoll BR, Tooredman JB, Capen D, di Tomaso E, Jain RK: Pathology: Cancer cells compress intratumour vessels. *Nature* 2004;427:695.
  - 95 Mason KA, Kishi K, Hunter N, Buchmiller L, Akimoto T, Komaki R, Milas L: Effect of docetaxel on the therapeutic ratio of fractionated radiotherapy in vivo. *Clin Cancer Res* 1999;5:4191-4198.
  - 96 Kabbinavar FF, Hurwitz HI, Yi J, Sarkar S, Rosen O: Addition of bevacizumab to fluorouracil-based first-line treatment of metastatic colorectal cancer: Pooled analysis of cohorts of older patients from two randomized clinical trials. *J Clin Oncol* 2009;27:199-205.
  - 97 Miller K, Wang M, Gralow J, Dickler M, Cobleigh M, Perez EA, Shenkier T, Cella D, Davidson NE: Paclitaxel plus bevacizumab versus paclitaxel alone for metastatic breast cancer. *N Engl J Med* 2007;357:2666-2676.
  - 98 Hurwitz H, Fehrenbacher L, Novotny W, Cartwright T, Hainsworth J, Heim W, Berlin J, Baron A, Griffing S, Holmgren E, Ferrara N, Fyfe G, Rogers B, Ross R, Kabbinavar F:

Bevacizumab plus irinotecan, fluorouracil, and leucovorin for metastatic colorectal cancer.

*N Engl J Med* 2004;350:2335-2342.

- 99 Sandler A, Gray R, Perry MC, Brahmer J, Schiller JH, Dowlati A, Lilenbaum R, Johnson DH: Paclitaxel-carboplatin alone or with bevacizumab for non-small-cell lung cancer. *N Engl J Med* 2006;355:2542-2550.

## **VITA**

Ricardo Hugo Alvarez was born in Fray Luis Beltran, Patagonia-Argentina on January 27, 1964, the son of Fanny D. Roldán J.D. and Ricardo Alvarez, M.D. After completing his work at Nicolas Avellaneda High School, Houston, Texas in 1984, she entered Universidad Nacional de La Plata in La Plata, Argentina. He received the degree of Medical Doctor in March, 1990. For the next four years, she worked as an Internal Medicine Resident at Centro Oncológico de Excelencia, Fundación José Maria Mainetti, Gonnet, Argentina. In 2004 he entered The University of Texas at Houston and completed the Internal medicine Residency in 2006. In July of 2009, after complete his fellowship in Hematology and Oncology, he started as Assistant Professor of Medicine at Breast Medical Oncology Department, MD Anderson Cancer Center. In July of 2007 he entered The University of Texas Health Science Center at Houston Graduate School of Biomedical Sciences.

Permanent address:

3807 Sun Valley Drive

Houston, Texas 77025